Chemistry
A European
Journal

Chemistry Europe
European Chemical Societies Publishing

Accepted Article

Title: Development of Pyridothiophene Compounds for PET Imaging of α-Synuclein

Authors: Anna Pees, Junchao Tong, Saritha Birudaraju, Yogeshkumar S. Munot, Steven H. Liang, Dinahlee Saturnino Guarino, Robert Mach, Chester A. Mathis, and Neil Vasdev

To be cited as: *Chem. Eur. J.* **2024**, e202303921

Link to VoR: https://doi.org/10.1002/chem.202303921

WILEY VCH

10.1002/chem.202303921

WILEY VCH

RESEARCH ARTICLE

Development of Pyridothiophene Compounds for PET Imaging of α-Synuclein

Anna Pees,[a] Junchao Tong,[a] Saritha Birudaraju,[b] Yogeshkumar S. Munot,[b] Steven H. Liang,[c] Dinahlee Saturnino Guarino,[d] Robert H. Mach,[d] Chester A. Mathis*[e] and Neil Vasdev*[a,f]

[a] Dr. A. Pees, Dr. J. Tong, Dr. N. Vasdev
Azrieli Centre for Neuro-Radiochemistry, Brain Health Imaging Centre, Campbell Family Mental Health Research Institute, Centre for Addiction and Mental Health (CAMH), Toronto, ON M5T 1R8, Canada;

[b] Dr. S. Birudaraju, Dr. Y. S. Munot
Sai Life Sciences Ltd., Hyderabad, Telangana, India-500078;

[c] Dr. S. H. Liang
Department of Radiology and Imaging Sciences, Emory University, Atlanta, Georgia 30322, United States;

[d] D. Saturnino Guarino, Dr. R. H. Mach
Department of Radiology, Perelman School of Medicine, University of Pennsylvania, 1012, 231 S. 34th Street, Philadelphia, Pennsylvania 19104-6323, United States;

[e] Dr. C. A. Mathis
Department of Radiology, University of Pittsburgh, Pittsburgh, Pennsylvania 15213, United States;
E-mail: mathisca@upmc.edu

[f] Dr. N. Vasdev
Department of Psychiatry, University of Toronto, Toronto, ON M5T-1R8, Canada;
Email: neil.vasdev@utoronto.ca

Supporting information for this article is given via a link at the end of the document.

Abstract: Aggregated α-synuclein (α-syn) protein is a pathological hallmark of Parkinson's disease (PD) and Lewy body dementia (LBD). Development of positron emission tomography (PET) radiotracers to image α-syn aggregates has been a longstanding goal. This work explores the suitability of a pyridothiophene scaffold for α-syn PET radiotracers, where 47 derivatives of a potent pyridothiophene (asyn-44; K_d = 1.85 nM) were synthesized and screened against [^{3}H]asyn-44 in competitive binding assays using post-mortem PD brain homogenates. Equilibrium inhibition constant (K_i) values of the most potent compounds were determined, of which three had K_i's in the lower nanomolar range (12-15 nM). An autoradiography study confirmed that [^{3}H]asyn-44 is promising for imaging brain sections from multiple system atrophy and PD donors. Fluorine-18 labelled asyn-44 was synthesized in 6±2% radiochemical yield (decay-corrected, n=5) with a molar activity of 263±121 GBq/μmol. Preliminary PET imaging of [^{18}F]asyn-44 in rats showed high initial brain uptake (>1.5 standardized uptake value (SUV)), moderate washout (~0.4 SUV at 60 min), and low variability. Radiometabolite analysis showed 60-80% parent tracer in the brain after 30 and 60 mins. While [^{18}F]asyn-44 displayed good *in vitro* properties and acceptable brain uptake, troublesome radiometabolites precluded further PET imaging studies. The synthesis and *in vitro* evaluation of additional pyridothiophene derivatives are underway, with the goal of attaining improved affinity and metabolic stability.

Introduction

Parkinson's disease (PD), Lewy body dementia (LBD) and multiple system atrophy (MSA) are diseases characterized by the presence of pathological α-synuclein (α-syn) aggregates and are therefore termed α-synucleinopathies.[1,2] α-Syn is a small presynaptic protein of 140 amino acids. In its physiological state, α-syn is unfolded, soluble, and can be found abundantly throughout the central nervous system (CNS). While its exact function is unknown it is purported that α-syn plays a role in synaptic plasticity.[3,4] In α-synucleinopathies, α-syn forms insoluble aggregates which are stabilized by a ß-sheet structure.[5,6] In PD and LBD, these aggregates are found in neuronal cell bodies (Lewy bodies) as well as axons and dendrites (Lewy neurites), with their distribution depending on the disease type and state. In MSA, the α-syn aggregates present as filamentous inclusions in oligodendrocytes (glia cell inclusions).[7,8] Typically, α-syn aggregation starts at the brain stem regions and spreads throughout the brain as the disease progresses. In this process, aggregated α-syn acts as a prion-like protein and seeds further aggregation of native α-syn.[9–11]

Since disease progression correlates with the accumulation of aggregated α-syn, there is a tremendous interest in developing positron emission tomography (PET) radiotracers targeting α-syn as a biomarker for PD, LBD and MSA.[5] Such a radiotracer would be valuable for target engagement studies, and to serve in the early diagnosis of α-synucleinopathies as well as in patient stratification for α-syn-targeted therapy.[12,13] Consequently, numerous PET tracers targeting α-syn have been developed.[4] However, to date, none of these tracers have proven ideal for PET imaging of PD patients.[14] During the preparation of this manuscript, the development of an α-syn PET radiopharmaceutical was reported, [^{18}F]ACI-12589, which bound to brain regions affected by α-synuclein pathology in patients with MSA; however, there was limited binding in PD.[15]

The development of α-syn PET tracers for PD remains to be amongst the greatest challenges in PET neuroimaging and is

10.1002/chem.202303921

hampered by several factors: First, the density of aggregated α-syn is low; about 10-50 times lower than the density of other protein aggregates such as amyloid beta (Aß). Therefore, a successful tracer needs to have a very high binding affinity (likely <1 nM) to increase the specific binding signal. Furthermore, the characteristic ß-sheet structure of aggregated α-syn is shared with other protein aggregates such as Aß and tau. Since α-syn accumulation is often accompanied by Aß and tau aggregation, it is imperative that the α-syn radiotracer has a high selectivity over these targets (at least 30–50 fold) in addition to other CNS targets. Another challenge is the intracellular location of the α-syn aggregates which requires the radiotracer to cross both the blood-brain barrier as well as cell membranes.[13,14,16] A recent review by Korat *et. al*. discusses these and other challenges in detail and gives a comprehensive list of suggested success criteria for α-syn PET tracers.[4]

The goal of the present work is to address the need for an α-syn PET radiotracer by further exploring a lead compound based on a pyridothiophene scaffold. This scaffold was disclosed in a patent by AC Immune from a heterogenous class of bicyclic compounds that were assayed for binding to α-syn and Aß plaques.[17] (*R*)-5-(6-(3-Fluoropyrrolidin-1-yl)pyridin-3-yl)-2-(pyridin-3-yl)thieno[3,2-b]pyridine (asyn-44; Figure 1) was shown to be potent (α-syn K_d = 9 nM; consistent with our assays) and had negligible staining of Aß plaques.[17] In the present study, we synthesized 47 derivatives of asyn-44 and screened them against [^{3}H]asyn-44 in competitive binding assays using post-mortem PD brain homogenates. K_i values of the most potent compounds were determined. We also synthesized [^{18}F]asyn-44 and evaluated this lead compound in healthy rats as a potential PET radiotracer for α-syn.

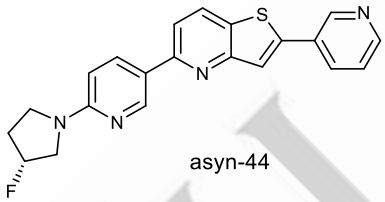

Figure 1. Structure of asyn-44.

Results and Discussion

Chemistry

A library of pyridothiophenes was synthesized by varying R and R´ substituents of the scaffold, resulting in four subclasses (I-IV) of compounds (Figure 2). In order to access the compounds of subclass I (Scheme 1), the commercially available pyridothiophene core **1** was cross-coupled with commercially available (6-fluoropyridin-3-yl)boronic acid in a Suzuki-Miyaura reaction to obtain **2** with a yield of 58.8%. After radical bromination with *N*-bromosuccinimide (87.5% yield)**,** the resulting compound **3** was subjected to Suzuki-Miyaura coupling with aryl boronic esters to obtain compounds **4-7** in yields ranging from 4 to 15%.

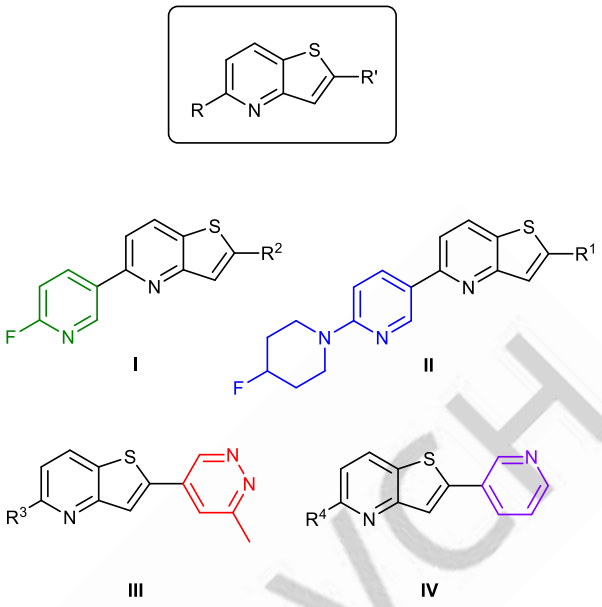

Figure 2. General structure and four subclasses of pyridothiophenes.

To access compounds of subclass II, **2** was reacted with 4-fluoropiperidine hydrochloride, followed by bromination with *N*-bromosuccinimide to obtain **9** in 30% isolated yield over two steps (Scheme 2). Compound **9** was further derivatized into a variety of compounds. These were mostly obtained via a palladium-catalysed cross- coupling reaction with aryl boronic acids (compounds **10-25**). Buchwald-Hartwig amination of **9** with three primary amines yielded compounds **26-28**. Pseudo-halogen exchange of **9** with CuCN in DMF yielded 23% of cyano-compound **29**. Further expansion of the library was achieved by reacting **9** with carbon monoxide to form the ethyl ester **30** with a yield of 81%, which served as an intermediate in the synthesis of five additional derivatives, **31-35** (Scheme 3). To access **31** and **32**, **30** was hydrolysed to **31** (92%) and subsequently reacted with dimethylamine hydrochloride to form the amide **32** (38%). Reaction of **30** with dimethylamine directly led to the formation of **33** (52%). **34** was synthesized by reduction of **30** with lithium aluminium hydride (22%), which was then methylated with methyl iodide in presence of sodium hydride, yielding 48% of **35.**

Derivatives of subclass III were obtained via compound **37**. **37** was synthesized in two steps from **1**, which was previously obtained during the synthesis of subclass I derivatives: **1** was brominated by use of elemental bromine and *n*-butyllithium, followed by palladium catalyzed cross-coupling with 3-methyl-5-Bpin-pyridazine (Scheme 4). Compound **37** was then further coupled with boronic acid pinacol esters under palladium catalysis to form compounds **38-41**. Boronic acid pinacol esters were obtained by Buchwald-Hartwig amination of the dihalogenated arenes with corresponding amines and subsequent Miyaura borylation. Buchwald-Hartwig amination of **37** yielded compounds **42** and **43**.

10.1002/chem.202303921
WILEY VCH

RESEARCH ARTICLE

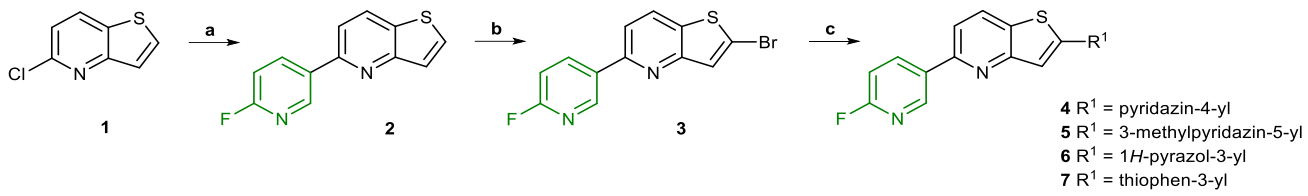

Scheme 1. Synthesis of subclass I derivatives; **a** (6-fluoropyridin-3-yl)boronic acid, K_2CO_3 , Pd(dppf)Cl_2•CH_2Cl_2, H_2O:dioxane, degassed N_2, 80-90 °C, 6 h; **b** NBS, AIBN, CCl_4, 100 °C; **c** Ar-BPin, Pd(dppf)Cl_2•CH_2Cl_2, Cs_2CO_3, 1,4-dioxane, H_2O.

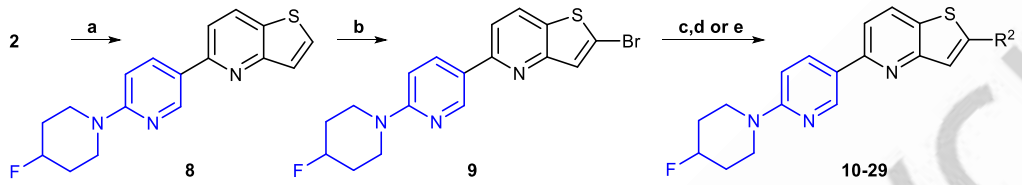

via conditions **c**

10 R^2 = 1*H*-pyrazol-4-yl
11 R^2 = 1-methylpyrazol-4-yl
12 R^2 = thiophen-3-yl
13 R^2 = 3-methylpyridazin-5-yl
14 R^2 = pyrimidin-5-yl
15 R^2 = pyridazin-4-yl
16 R^2 = 2-methylpyridin-4-yl
17 R^2 = pyridin-4-yl
18 R^2 = phenyl
19 R^2 = 3-methylpyridin-5-yl
20 R^2 = 2-fluoropyridin-4-yl
21 R^2 = 2-fluoropyridin-3-yl
22 R^2 = quinolin-3-yl
23 R^2 = 3-methoxyphenyl
24 R^2 = cyclopropyl
25 R^2 = prop-1-en-2-yl

via conditions **d**

26 R^2 = *N*-(oxetan-3-yl)amine
27 R^2 = *N*-(tetrahydro-2*H*-pyran-4-yl)amine
28 R^2 = *N*-(pyridazin-4-yl)amine

via conditions **e**

29 R^2 = CN

Scheme 2. Synthesis of subclass II derivatives (part I); **a** 4-fluoropiperidine·HCl, K_2CO_3, DMSO, 100 °C, 18 h.; **b** NBS, $CHCl_3$, 0 °C - rt, 2 h; **c** Ar-B$(OH)_2$, PdCl$_2$(dppf)•CH_2Cl_2, Cs_2CO_3, Dioxane/H_2O, 70-100 °C; **d** R-NH_2, $Pd_2(dba)_3$, BINAP, *t*-BuONa, toluene, 100 °C; **e** CuCN, DMF, 120 °C, 18 h.

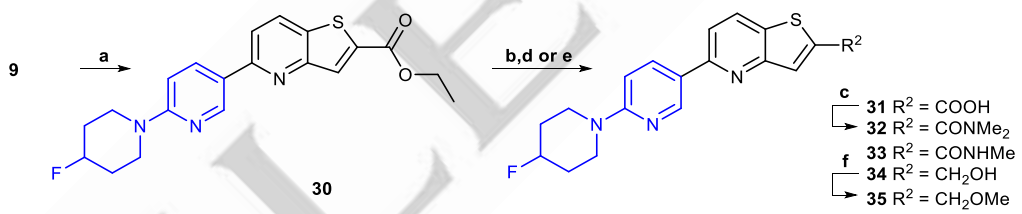

Scheme 3. Synthesis of subclass II derivatives (part II); **a** CO (g), $Pd(OAc)_2$, DPPF, TEA, EtOH-DMF (4:1), Steel bomb, 100°C, 16 h; **b** LiOH•H_2O, THF/H_2O, RT, 6 h; **c** $NHMe_2$•HCl, DIPEA, HATU, DMF, RT, 16 h; **d** 33% $MeNH_2$/Ethanol, 90 °C, 16 h; **e** $LiAlH_4$, THF, RT, 3 h; **f** MeI, NaH, DMF, 0 °C- RT, 3 h.

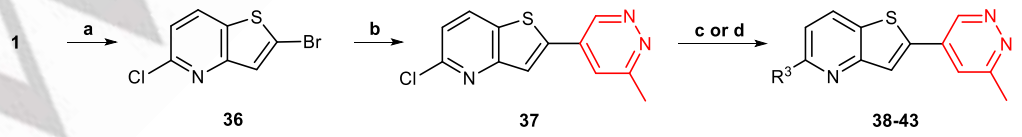

via conditions **c**

38 R^3 = (2-fluoro-4-(4-fluoropiperidin-1-yl)phenyl
39 R^3 = 4-(4-fluoropiperidin-1-yl)-2-methoxyphenyl
40 R^3 = 2-(4-fluoropiperidin-1-yl)pyrimidin-5-yl
41 R^3 = 2-fluoropyridin-4-yl

via conditions **d**

42 R^3 = 4-(4-fluorophenyl)piperidin-1-yl
43 R^3 = 4-(4-fluoropiperidin-1-yl)piperidin-1-yl

Scheme 4. Synthesis of subclass III derivatives; **a** 1.2.5 M *n*-BuLi, Br_2, THF, -78 °C → RT, 2 h; **b** 3-methyl-5-BPin-pyridazine, Pd(dppf)Cl_2, Cs_2CO_3, dioxane, H_2O, 90 °C, MW, 40 min; **c** R-BPin, Pd(dppf)Cl_2, Cs_2CO_3, dioxane, H_2O, 100 °C, MW; **d** $Pd_2(dba)_3$, BINAP, *t*-BuONa, Toluene, 100 °C, MW, 40 min.

10.1002/chem.202303921

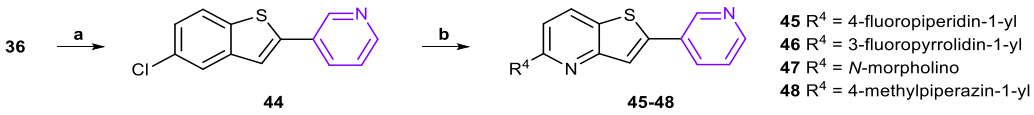

Scheme 5. Synthesis of subclass IV derivatives (part I); **a** Pyridin-3-ylboronic acid, $PdCl_2dppf•CH_2Cl_2$, Cs_2CO_3, dioxane/H_2O; **b** Amines, K_2CO_3, DMSO, 100 °C, 12 h.

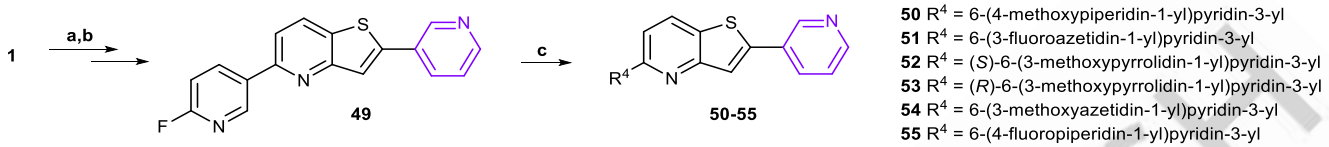

Scheme 6 Synthesis of subclass IV derivatives (part II); **a** Nitrogen nucleophile, *n*-BuOH, DIPEA, 200 °C, 1h, MW.

Derivatives of subclass IV were synthesized via two different routes. Derivatives **45-48** were synthesized in two steps from **36**: First, **36** was subjected to a Suzuki-Miyaura coupling with pyridin-3-ylboronic acid to form compound **44**, which was subsequently reacted with a variety of amines (free base or hydrogen chloride salt) to yield the respective derivative (Scheme 5). To access derivatives **50-55**, compound **49** was synthesized in two steps from **1** and subsequently coupled to the respective nitrogen nucleophile to yield **50-55** (Scheme 6).

Radiochemistry

[^{3}H]Asyn-44 (1.5 GBq/µmol, 36 MBq/mL; Figure 3) was labelled with tritium gas from the respective dibromo precursor at Novandi Chemistry AB (Södertälje, Sweden).

The radiofluorination of asyn-44 for PET imaging studies was carried out by nucleophilic substitution (S_N2) reaction of the corresponding toluenesulfonate precursor (synthesis see SI) with [^{18}F]fluoride (Scheme 7), using the reaction conditions previously reported for [^{18}F]fluoropyrolidines,[18] with minor modifications. Aqueous [^{18}F]fluoride was obtained from the cyclotron, azeotropically dried with potassium carbonate and 4,7,13,16,21,24-hexaoxa-1,10-diazabicyclo[8.8.8]hexacosane (Kryptofix® 222), and reacted with the toluenesulfonate precursor at 100 °C in DMSO for 10 min. After semi-preparative HPLC purification and formulation in ethanolic saline solution, [^{18}F]asyn-44 was obtained in a total synthesis time of 1 hour with a radiochemical purity of >95%, a radiochemical yield (RCY) of 6±2% (decay-corrected, n=5), and a molar activity of 263±121 GBq/µmol. As the RCY was sufficient for subsequent imaging studies, no further optimization was carried out. The $logD_{7.4}$ of [^{18}F]asyn-44 was measured using the shake-flask procedure[19] to 4.16±0.04 (n=8). This value is slightly higher than the ideal range suggested by blood-brain barrier permeability prediction models (1.5-3.5)[20] but not unusual for brain-penetrating PET tracers.

In vitro evaluation of asyn-44

[^{3}H]Asyn-44 was characterized *in vitro* to determine its suitability as a lead for α-syn PET tracer development. First, the equilibrium dissociation constant (K_d), and maximal number of binding sites (B_{max}) were determined in PD and Alzheimer's disease (AD) tissue. It was found that asyn-44 bound with high affinity in PD tissues (K_d=1.85±0.38 nM, B_{max}=55±9 nM, n=3) and was much less potent in AD tissues (K_d=170±60 nM, B_{max}=420±200 nM, n=3).

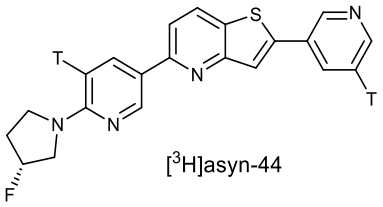

Figure 3. Structure of tritium labelled asyn-44.

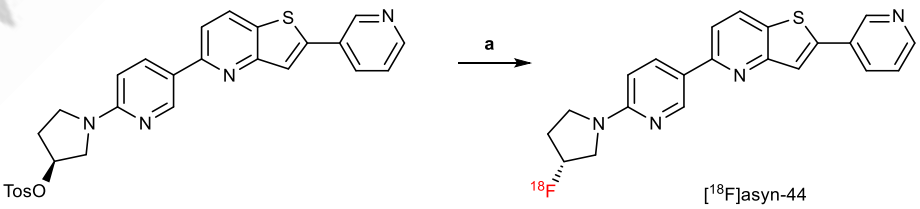

Scheme 7. Radiosynthesis of [^{18}F]asyn-44; **a** [^{18}F]fluoride, K_2CO_3, Kryptofix®222, DMSO, 100 °C, 10 min.

10.1002/chem.202303921

Table 1. K_i values (n =1) of [^{3}H]asyn-44 and various tau ligands in AD brain homogenates.

Tau ligand	K_i (nM)
PI-2620	>10,000
APN-1607	>10,000
OXD-2115	>10,000
MK-6240	4600

Additional binding assays were conducted in AD tissue homogenates to assess the affinity of asyn-44 in competition with [^{3}H]PiB binding to aggregated Aβ. The K_i of asyn-44 versus [^{3}H]PiB in AD brain homogenate was 9600±800 nM (n=3), indicating a relatively poor affinity of asyn-44 for the PiB binding site on aggregated Aβ. To assess the affinity of asyn-44 for different tau binding sites, [^{3}H]asyn-44 was screened against four tau-PET ligands, PI-2620, APN-1607 (a.k.a. PM-PBB3), OXD-2115 (a.k.a. CBD-2115) and MK-6240 (Table 1). K_i values were in the millimolar range or greater, indicating low affinity to all of their respective tau binding sites.

An autoradiography study was carried out with [^{3}H]asyn-44 in brain sections from MSA and PD donors. [^{3}H]Asyn-44 gave a clear signal overlapping with α-syn neuropathology visualized using anti-pS129 α-syn immunohistochemistry (IHC). The specificity of the pathological α-syn signal was confirmed by the extent of co-localization with pS129 IHC as well as its displacement by an excess of unlabelled asyn-44. In contrast to the synucleinopathy samples, [^{3}H]asyn-44 showed only weak binding in AD, progressive supranuclear palsy (PSP), corticobasal degeneration (CBD) pathologies and control case. Binding to the non-demented control case was due to the presence of a-syn inclusions. Selectivity over pathological tau was further assessed by IHC for misfolded tau and no clear co-localization between tau inclusions by IHC and [^{3}H]asyn-44 autoradiographic signal was observed.

In vitro evaluation of the pyridothiophene derivatives

The synthesized derivatives were evaluated *in vitro* to determine the most promising compounds for use as α-syn PET radiotracers. Most of the compounds were initially screened in a two-point assay, similarly to our previous report.[21] The objective of this screen was to determine which structural derivatives displaced [^{3}H]aysn-44 in a dose-dependent manner and to select the leads with the most promise for full competition binding assays. The compounds were screened against [^{3}H]asyn-44 in human PD tissue homogenates at two concentrations (30 and 300 nM). Figure 5 shows a heat map of the screening results, with exact values in the SI (Table S1). Even though many compounds showed good inhibition (<50% remaining bound [^{3}H]asyn-44) at 300 nM concentration, only a few showed good inhibition at 30 nM.

For compounds with very good inhibition (<30% bound [^{3}H]asyn-44) at 300 nM and moderate to good inhibition (<70% bound [^{3}H]asyn-44) at 30 nM, as well as for compounds that had not been screened in the two-point assay, we determined the full competition binding curve to calculate their equilibrium inhibition constant (K_i). The results of the compounds with a K_i < 50 nM are shown in Table 2. The only compounds in the lower nanomolar range were **13** (K_i 12.1 nM), **55** (K_i 12.2 nM) and **51** (K_i 14.6 nM). These compounds are structurally very similar to the lead asyn-44: They had minor modifications at the fluoropyrrolidine ring and, in case of **13**, a small modification at the pyridine ring. However, none of these three compounds showed higher binding affinity than the lead compound, and we proceeded with asyn-44 for further *in vivo* characterization.

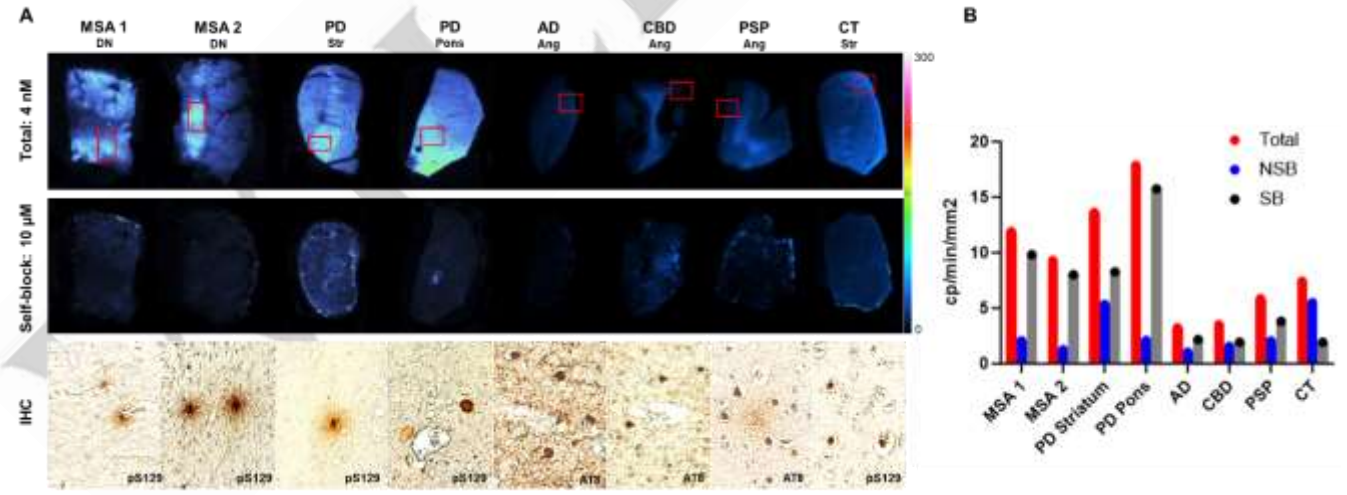

Figure 4. *In vitro* evaluation of [^{3}H]asyn-44. **A** Autoradiography of [^{3}H]asyn-44 in MSA (dentate nucleus (DN)), PD (striatum (Str), pons), AD (angular gyrus (Ang)), CBD (Ang), PSP (Ang) and control (Str) tissue, total binding (upper panel) and self-blocked (middle panel); lower panel: matching IHC with anti-pS129; **B** Total, non-specific (NSB) and specific (SB) binding of [^{3}H]asyn-44 in MSA, PD, AD, DBD, PSP and CT tissue.

10.1002/chem.202303921

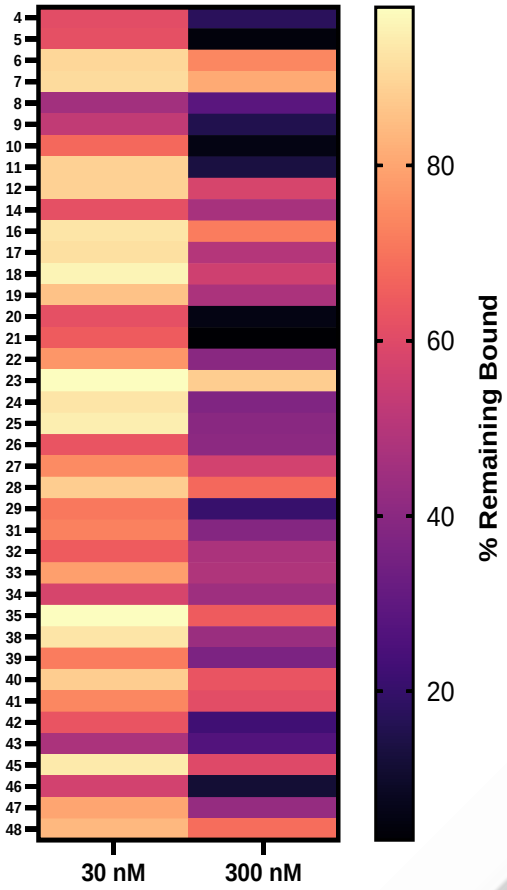

Figure 5. Heat map of the two-point screening results.

Table 2. Ki's of selected derivatives in PD tissue.

Compound	K_i (nM)
46	29.6
10	32.0
21	37.6
20	46.2
9	30.7
8	31.9
15	26.4
13	12.1
55	12.2
51	14.6
50	48.9

Overall, we found that only limited modifications of the lead structure retained high affinity to the target. The ring size of the 3-fluoropyrrolidinyl group could be increased or decreased; the fluorine atom was, however, important to retain high affinity. This is probably due to the "fluorine effect" where the electrochemical effect of fluorine influences physicochemical properties of a compound.[22,23] The terminal pyridyl group was modified, however, nitrogen-bearing heterocyles generally retained the highest affinities. An exception is replacement of the pyridyl group by thiophene, bromide or cyanide, which also resulted in moderate-high affinity.

The limited success to synthesize compounds for α-syn with sub-nM affinity can be attributed to α-syn being an intrinsically disordered protein which can adopt a range of structural conformations. The availability of high-resolution X-ray crystal structures of α-syn aggregates is limited, which further hampers a structure-based drug design approach. Therefore, it is difficult to predict which structural modifications on the ligands will improve binding.

In vivo evaluation of [^{18}F]asyn-44

To investigate if asyn-44 is a suitable candidate for the imaging of α-syn *in vivo*, we conducted preliminary PET imaging studies with [^{18}F]asyn-44 in male and female wild-type rats. After intravenous (i.v.) administration of the tracer, the radioactivity in the entire brain peaked at an initial maximum standardized uptake value (SUV; semiquantitative measure of tracer uptake, defined as the activity concentration in a region of interest normalized to the total injected amount of radioactivity per body weight) of >1.5 within 5 minutes of injection, gradually decreasing to 0.4 SUV over the course of the 120-minute PET scan (Figure 6). These findings revealed that [^{18}F]asyn-44 has good brain permeability and moderate brain clearance, which are suitable characteristics for a PET tracer targeting α-asyn. No difference between sexes was observed in our preliminary study.

A radiometabolite studies of [^{18}F]asyn-44 was carried out to assess potential brain-penetrant metabolites which could confound PET imaging.

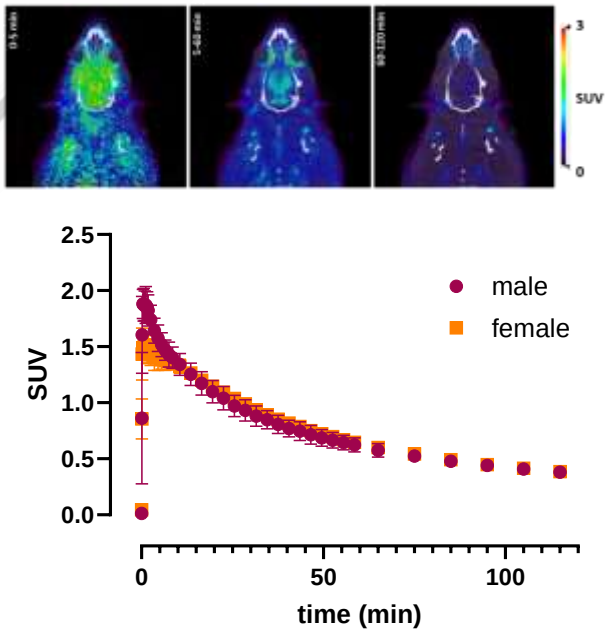

Figure 6. *In vivo* brain PET study of [^{18}F]asyn-44 in rats; dynamic PET images were obtained for 120 min. Top: Representative example of summed images (0−5, 5-60, and 60-120 mins); Bottom: Time-activity curves of [^{18}F]asyn-44 in whole brain of male and female rats (n = 3 each).

Table 3. Results of the metabolite study; % intact tracer after 30 and 60 minutes; n=3 except for *(n=2).

	Plasma %		Brain %	
	30 min	60 min	30 min	60 min
Female	25±15	21±10*	72±6	62±1*
Male	32±15	13±9	57±32	47±25

Blood plasma as well as brain homogenates were analysed 30 and 60 minutes post injection of the radiotracer (Table 3) which revealed a low plasma stability of the tracer for both sexes with less than 50% intact tracer after 30 minutes. While this is not necessarily a problem for brain tracers, radiometabolites were identified in the brain homogenates at a higher rate than what would be expected in a non-perfused brain. In females 30-40% radiometabolites (polar and lipophilic) were present after 30-60 minutes, and males showed even higher average percentage of radiometabolites at both timepoints. While the polar metabolites were likely formed in the brain, the lipophilic metabolites may also cross the blood brain barrier from the plasma into the brain (SI, Figures S7 and S8). To avoid the formation of brain-penetrant radiolabelled metabolites in future derivatives, alternative labelling sites could be considered and/or structural modifications of the scaffold need to be explored.[24,25] Based on common metabolic reactions, the lipophilic metabolites might result from oxidation of the *N*-heterocycles, either at the carbon or nitrogen atoms. A potential strategy for the future development of asyn-44 derivatives could be to reduce likelihood of oxidation by decreasing the electron density in the *N*-heterocycles (e.g. through introduction of more nitrogen atoms), to explore radiolabelling at the central or terminal rings, or by attempting to block metabolic positions by introducing suitable substituents.[26,27]

Conclusion

This work demonstrates that asyn-44 is a potent (K_d = 1.85 nM) lead compound and the pyridothiophene scaffold is promising for the development of an α-syn PET tracer in both PD and MSA. While [^{18}F]asyn-44 exhibited favourable *in vitro* and *in vivo* characteristics for neuroimaging, the presence of radiometabolites in rat brain precluded further PET imaging studies. Our future efforts are focused on the synthesis and *in vitro* evaluation of additional derivatives of asyn-44 with the goal of attaining improved affinity and metabolic stability.

Experimental

General

Ligands **50-55** were provided by MedChem Imaging, Inc. (Boston, USA) with >95% purity. All other ligands and labelling precursors were provided by Sai Life Sciences Ltd. (Telangana, India) with >90% purity. [^{3}H]Asyn-44 (1.5 GBq/μmol, 36 MBq/mL; Figure 3) was labelled with tritium gas from the respective dibromo precursor at Novandi Chemistry AB (Södertälje, Sweden). All other chemicals and reagents were obtained from commercial vendors and were used as received without further purification. [^{18}F]Fluoride was produced with a MC-17 cyclotron (Scanditronix, Sweden) from an oxygen-18 enriched water target. Analytical HPLC was performed on a 1260 Infinity II HPLC system (Agilent, CA) with a M177 γ-radiation detector (Ludlum Instruments, TX) connected in series after the UV detector. Radiochemistry was performed in lead-shielded hot cells in a laboratory designed to handle radioactive material. The work was carried out in accordance with the radiation protection guidelines and regulations from the Canadian Nuclear Safety Commission and internal safety policies and procedures. Animal studies were carried out in accordance with the guidelines put forth by the institutional animal care and use committees at CAMH (Protocol 891).

Synthesis of asyn-44 derivatives

5-(6-Fluoropyridin-3-yl)thieno[3,2-b]pyridine 2: To the stirred solution of 5-chlorothieno[3,2-b]pyridine **1** (4 g, 23.8 mmol, 1 eq) and (6-fluoropyridin-3-yl)boronic acid **2** (4.02 g, 28.5 mmol, 1.2 eq) in 1,4-dioxane (6 mL) and water (0.1 mL) was added K_2CO_3 (4.9 g, 35.7 mmol, 1.5 eq). The reaction mixture was purged with argon gas for 10 min. Then $Pd(PPh_3)_4$ (2.74 g, 2.38 mmol, 0.1 eq) was added at room temperature and the reaction mixture was stirred at 100 °C for 40 min under microwave irradiation. The progress of the reaction was monitored by TLC and LCMS. The reaction mixture was filtered through celite, washed with DCM, concentrated under reduced pressure and purified by Combi-flash column chromatography. Pure fractions were concentrated under reduced pressure to get 5-(6-fluoropyridin-3-yl)thieno[3,2-b]pyridine **2** (4.5 g, 83%).

2-Bromo-5-(6-fluoro-3-pyridyl)thieno[3,2-b]pyridine 3: To a solution of 5-(6-fluoro-3-pyridyl)thieno[3,2-b]pyridine **2** (600 mg, 2.60 mmol, 1 eq) in CCl_4 (10 mL) was added NBS (2.32 g, 13.04 mmol, 5 eq) and AIBN (90 mg, 0.52 mmol, 0.2 eq). The resulting reaction mixture was heated at 100-110 °C for 18 h. The progress of the reaction was monitored by TLC and LCMS. After completion, the reaction mixture was concentrated *in vacuo* and purified by combi flash chromatography (15% EtOAc/Heptane) to afford 2-bromo-5-(6-fluoro-3-pyridyl)thieno[3,2-b]pyridine **3** (700 mg, 87.5 %) as an off white solid.

General procedure 4-7: To a stirred solution of 2-bromo-5-(6-fluoropyridin-3-yl)thieno[3,2-b]pyridine **3** (1 eq) and the respective aryl boronic ester (1.5 eq) in 1,4-dioxane/water (4:1) (5-10 mL) was added Cs_2CO_3 or *t*-BuONa (2.5 eq). The reaction mixture was degassed with nitrogen gas for 10-15 min, then $Pd(dppf).CH_2Cl_2$ (0.1 eq) was added, and the mixture was again degassed with nitrogen gas for 10-15 min. Then, the mixture was heated at 110 °C for 1 h in a microwave. The progress of the reaction was monitored by TLC and LCMS. After completion, the reaction mixture was cooled to RT, filtered through celite and washed with EtOAc. The organic layer was dried over Na_2SO_4 and concentrated *in vacuo*. The crude was purified by preparative HPLC to afford the product (4-15%).

5-(6-(4-Fluoropiperidin-1-yl)pyridin-3-yl)thieno[3,2-b]pyridine 8: DIPEA (13.1 mL, 32.4 mmol, 3 eq) was added to the stirred solution of 5-(6-fluoropyridin-3-yl)thieno[3,2-b]pyridine **3** (2.5 g, 10.8 mmol, 1 eq) and 4-fluoropiperidine.hydrogen chloride (1.8 g,

10.1002/chem.202303921

12.9 mmol, 1.2 eq) in *n*-butanol at room temperature and the reaction mixture was stirred at 200 °C for 1 h under microwave irradiation. The progress of the reaction was monitored by TLC and LCMS. The reaction mixture was concentrated under reduced pressure, diluted with EtOAc and washed with water and brine solution. The combined organic layer was dried over Na_2SO_4, concentrated under reduced pressure and purified by Combi-flash column chromatography. Pure fractions were concentrated under reduced pressure to get 5-(6-(4-fluoropiperidin-1-yl)pyridin-3-yl)thieno[3,2-b]pyridine **8** (2.1 g, 70%).

2-Bromo-5-(6-(4-fluoropiperidin-1-yl)pyridin-3-yl)thieno[3,2-b]pyridine 9: To the stirred solution of 5-(6-(4-fluoropiperidin-1-yl)pyridin-3-yl)thieno[3,2-b]pyridine **8** (2 g, 6.38 mmol, 1 eq) in THF was added 2M *n*-BuLi (4.79 mL, 9.58 mmol, 1.5 eq) at -78 °C. After stirring at the same temperature for 30 minutes, Br_2 (0.62 mL, 12.1 mmol, 1.9 eq) was added and the reaction mixture was stirred at RT for 2 h. The progress of the reaction was monitored by TLC and LCMS. The reaction mixture was quenched with NH_4Cl and $NaHCO_3$ solutions. The organic layer was extracted with EtOAc and the combined organic layers were dried over Na_2SO_4, concentrated under reduced pressure and purified by Combi-flash column chromatography. Pure fractions were concentrated under reduced pressure to get 2-bromo-5-(6-(4-fluoropiperidin-1-yl)pyridin-3-yl)thieno[3,2-b]pyridine **9** (1.1 g, 44%).

General procedure 16-19, 22-23: To the stirred solution of 2-bromo-5-(6-(4-fluoropiperidin-1-yl)pyridin-3-yl)thieno[3,2-b]pyridine **9** (1 eq) and the respective boronic acid (1.2 eq) in 1,4-dioxane (3 mL) and water (0.1 mL) was added Cs_2CO_3 (1.5 eq). The reaction mixture was purged for 10 min with argon gas. Then, Pd(dppf)Cl_2 (0.1 eq) was added at room temperature and the reaction mixture was stirred at 100 °C for 45 min under microwave irradiation. The progress of the reaction was monitored by TLC and LCMS. The reaction mixture was filtered through celite and washed with DCM. The filtrate was concentrated under reduced pressure to get the crude compound, which was purified by Combi-flash column chromatography. Pure fractions were concentrated under reduced pressure to get the desired product.

General procedure 10-15, 20-21,24-25: To a stirred solution of 2-bromo-5-(6-(4-fluoropiperidin-1-yl)pyridin-3-yl)thieno[3,2-b]pyridine **9** (1 eq) and the respective boronic acid precursor (1.3-7 eq) in 1,4-dioxane/water (4:1) was added Cs_2CO_3 (2.5 eq). The reaction mixture was degassed with nitrogen gas for 15-30 mins, then Pd(dppf).CH_2Cl_2 (0.1 eq) was added, and the mixture was again degassed with nitrogen gas for 15-30 mins. The reaction was allowed to stir at 70-110 °C for 5-16 h. The progress of the reaction was monitored by TLC. After completion, the reaction mixture was cooled to RT, filtered through celite and washed with EtOAc. The organic layer was dried over Na_2SO_4, concentrated *in vacuo* and purified by combi flash column chromatography or preparative HPLC to afford the product.

General procedure 26-28: To the stirred solution of 2-bromo-5-(6-(4-fluoropiperidin-1-yl)pyridin-3-yl)thieno[3,2-b]pyridine **9** (1 eq) and R-NH_2 (1.2 eq) in toluene (6 mL) was added sodium *tert*-butoxide (3 eq). After stirring the reaction mixture for 10 min under argon gas purging, BINAP (0.15 eq) and $Pd_2(dba)_3$ (0.1 eq) were added at room temperature and the reaction mixture was stirred at 100 °C for 50 min under microwave irradiation. The progress of the reaction was monitored by TLC and LCMS. The reaction mixture was filtered through celite and washed with DCM. The filtrate was concentrated under reduced pressure to get the crude compound which was purified by Combi-flash column chromatography. Pure fractions were concentrated under reduced pressure to get the desired product.

5-(6-(4-Fluorocyclohexyl)pyridin-3-yl)thieno[3,2-b]pyridine-2-carbonitrile 29: To a solution of 2-bromo-5-(6-(4-fluoropiperidin-1-yl)pyridin-3-yl)thieno[3,2-b]pyridine **9** (100 mg, 0.25 mmol, 1 eq) in DMF (1 mL) was added CuCN (430 mg, 4.85 mmol, 19 eq) at RT. The resulting reaction mixture was heated at 120 – 140 °C for 36 h. The progress of reaction was monitored by TLC and LCMS. After completion, the reaction mixture was cooled to RT, quenched with water and extracted with 5% EtOAc (2 x 50 mL). The organic layer was dried over Na_2SO_4, concentrated *in vacuo* and purified by combi flash using 20% EtOAc/heptane to afford 5-(6-(4-fluorocyclohexyl)pyridin-3-yl)thieno[3,2-b]pyridine-2-carbonitrile **29** (20 mg, 23.0%) as a white solid.

Ethyl 5-(6-(4-fluoropiperidin-1-yl)pyridin-3-yl)thieno[3,2-b]pyridine-2-carboxylate 30: To a stirred solution of 2-bromo-5-(6-(4-fluoropiperidin-1-yl)pyridin-3-yl)thieno[3,2-b]pyridine **9** (500 mg, 1.27 mmol, 1 eq) in EtOH/CH_2Cl_2 (4:1) (13 mL) was added triethyl amine (0.53 mL, 3.82 mmol, 3 eq) at RT. The reaction mixture was degassed with argon for 30 mins, DPPF (211 mg, 0.38 mmol, 0.3 eq) and $Pd(OAc)_2$ (42 mg, 0.19 mmol, 0.15 eq) were added, and the mixture was further degassed with argon for 10 min. The reaction mixture was then allowed to stir at 100 °C in a steel bomb at 150 psi $CO_{(g)}$ pressure for 16 h. The progress of the reaction was monitored by TLC. After the completion of the reaction, the mixture was filtrated through celite, concentrated *in vacuo* and purified by Combi-flash column chromatography (20% EtOAc/heptane) to afford ethyl 5-(6-(4-fluoropiperidin-1-yl)pyridin-3-yl)thieno[3,2-b]pyridine-2-carboxylate **30** (400 mg, 81.4%) as a pale yellow gum.

5-(6-(4-Fluoropiperidin-1-yl)pyridin-3-yl)thieno[3,2-b]pyridine-2-carboxylic acid 31: To a stirred solution of ethyl 5-(6-(4-fluoropiperidin-1-yl)pyridin-3-yl)thieno[3,2-b]pyridine-2-carboxylate **30** (100 mg, 0.25 mmol, 1 eq) in THF/water (1:1) (6 mL) was added LiOH•H_2O (32 mg, 0.77 mmol, 3 eq) at RT. The reaction mixture was allowed to stir at RT for 6 h. The progress of the reaction was monitored by TLC. After the completion of the reaction, the reaction mixture was concentrated *in vacuo,* diluted with water and extracted with EtOAc. The aqueous layer was acidified with citric acid and extracted with DCM (2 x 10 mL). The combined organic layer was washed with water, dried over sodium sulfate and concentrated *in vacuo* to afford 5-(6-(4-fluoropiperidin-1-yl)pyridin-3-yl)thieno[3,2-b]pyridine-2-carboxylic acid **31** (85 mg, 91.6%) as a yellow solid.

5-(6-(4-Fluoropiperidin-1-yl)pyridin-3-yl)-*N,N*-dimethylthieno[3,2-b]pyridine-2-carboxamide 32: To a stirred solution of 5-(6-(4-fluoropiperidin-1-yl)pyridin-3-yl)thieno[3,2-b]pyridine-2-carboxylic acid **31** (75 mg, 0.20 mmol, 1 eq) and $MeNMe_2$.HCl (42 mg, 0.52 mmol, 2.5 eq) in DMF (5 mL) was added DIPEA (0.109 mL, 0.62 mmol, 3 eq) and HATU (159 mg, 0.41 mmol, 2 eq) at 0 °C. The resulting reaction mixture was allowed to stir at RT for 16 h. The progress of the reaction was monitored by TLC. After completion, the reaction mixture was

10.1002/chem.202303921

diluted with water and extracted using DCM (2 x 10 mL). The combined organic layer was washed with water and brine, dried over sodium sulfate and concentrated *in vacuo*. The crude was purified by preparative HPLC and the compound dried under lyophilisation to afford 5-(6-(4-fluoropiperidin-1-yl)pyridin-3-yl)-*N,N*-dimethylthieno[3,2-b]pyridine-2-carboxamide **32** (30 mg, 37.5%) as an off white solid**.**

5-(6-(4-Fluoropiperidin-1-yl)pyridin-3-yl)-*N*-methylthieno[3,2-b]pyridine-2-carboxamide 33: To a stirred solution of ethyl 5-(6-(4-fluoropiperidin-1-yl)pyridin-3-yl)thieno[3,2-b]pyridine-2-carboxylate **30** (100 mg, 0.25 mmol, 1 eq) in ethanol (3 mL) was added 33% methylamine in ethanol (10 mL) at RT. The reaction was allowed to stir at 90 °C for 16 h. The progress of the reaction was monitored by TLC. After completion, the reaction mixture was concentrated *in vacuo* and purified by preparative HPLC. After purification, the compound was dried under lyophilisation to afford 5-(6-(4-fluoropiperidin-1-yl)pyridin-3-yl)-*N*-methylthieno[3,2-b]pyridine-2-carboxamide **33** (50 mg, 52%) as a white solid.

(5-(6-(4-Fluoropiperidin-1-yl)pyridin-3-yl)thieno[3,2-b]pyridin-2-yl)methanol 34: To a stirred solution of ethyl 5-(6-(4-fluoropiperidin-1-yl)pyridin-3-yl)thieno[3,2-b]pyridine-2-carboxylate **30** (120 mg, 0.31 mmol, 1 eq) in THF (10 mL) was added $LiAlH_4$ (0.46 mL, 0.93 mmol, 3 eq) at 0 °C. The resulting reaction mixture was allowed to stir at RT for 3 h. The progress of the reaction was monitored by TLC and LCMS. After completion, the reaction mixture was quenched with ice cold water and extracted with EtOAc (2 x 15 mL). The combined organic layer was dried over Na_2SO_4, concentrated *in vacuo* and purified by combi flash column chromatography (20-25% EtOAc in heptane) to afford (5-(6-(4-fluoropiperidin-1-yl)pyridin-3-yl)thieno[3,2-b]pyridin-2-yl)methanol **34** (20 mg, 22.2%) as a pale yellow solid.

5-(6-(4-Fluoropiperidin-1-yl)pyridin-3-yl)-2-(methoxymethyl)thieno [3,2-b]pyridine 35: To a stirred solution of (5-(6-(4-fluoropiperidin-1-yl)pyridin-3-yl)thieno[3,2-b]pyridin-2-yl)methanol **35** (60 mg, 0.17 mmol, 1 eq) in DMF (5 mL) was added NaH (13 mg, 0.34 mmol, 2 eq) and MeI (0.016 mL, 0.26 mmol, 1.5 eq) at 0 °C. The resulting reaction mixture was allowed to stir at RT for 3 h. The progress of the reaction was monitored by TLC. After the completion of the reaction, ice cold water was added, and the mixture was extracted with EtOAc (2 x 10 mL). The organic layer was washed with water, dried over sodium sulfate and concentrated *in vacuo.* The crude was purified by combi-flash using 10% EtOAc/heptane to afford 5-(6-(4-fluoropiperidin-1-yl)pyridin-3-yl)-2-(methoxymethyl)thieno [3,2-b]pyridine **35** (30 mg, 48.3%) as a pale yellow solid**.**

2-Bromo-5-chlorothieno[3,2-b]pyridine 36: To the stirred solution of 5-chlorothieno[3,2-b]pyridine **1** (5.5 g, 32.3 mmol, 1 eq) in THF was added 2.5 M *n*-BuLi (19.4 mL, 48.5 mmol, 1.5 eq) at -78 °C. After stirring at -78 °C for 30 minutes, Br_2 (3.1 mL, 61.3 mmol, 1.9 eq) was added and the reaction mixture was stirred at RT for 2 h. The progress of the reaction was monitored by TLC and LCMS. The reaction mixture was quenched with NH_4Cl and $NaHCO_3$ solutions. The organic layer was extracted with EtOAc. The combined organic layer was dried over Na_2SO_4, concentrated under reduced pressure, and purified by Combi-flash column chromatography. Pure fractions were concentrated under reduced pressure to afford 2-bromo-5-chlorothieno[3,2-b]pyridine **36** (2.1 g, 26%).

5-Chloro-2-(6-methylpyridazin-4-yl)thieno[3,2-b]pyridine 37: To the stirred solution of 2-bromo-5-chlorothieno[3,2-b]pyridine **36** (1 g, 4.03 mmol, 1 eq) and 3-methyl-5-(4,4,5,5-tetramethyl-1,3,2-dioxaborolan-2-yl)pyridazine (1.06 g, 4.83 mmol, 1.2 eq) in 1,4-dioxane (10 mL) and water (1 mL) was added Cs_2CO_3 (1.9 g, 6.04 mmol, 1.5 eq). The reaction mixture was purged for 10 min with argon gas, followed by addition of $Pd(dppf)Cl_2$ (0.29 g, 0.40 mmol, 0.1 eq) at room temperature and stirring at 90 °C for 40 min under microwave irradiation. The progress of the reaction was monitored by TLC and LCMS. The reaction mixture was filtered through celite and washed with DCM. The filtrate was concentrated under reduced pressure and purified by Combi-flash column chromatography. Pure fractions were concentrated under reduced pressure to get 5-chloro-2-(6-methylpyridazin-4-yl)thieno[3,2-b]pyridine **37** (0.4 g, 38%).

General procedure 38-41: 5-Chloro-2-(6-methylpyridazin-4-yl)thieno[3,2-b]pyridine **37** (1 eq) and Cs_2CO_3 (1.5 eq) were added to a stirred solution of the respective boronic acid (1-1.2 eq) in 1,4-dioxane (3 mL) and water (0.1 mL). The reaction mixture was purged for 10 min with argon gas. $Pd(dppf)Cl_2$ (0.1 eq) was added at room temperature and the reaction mixture was stirred at 90-100 °C for 40-60 min under microwave irradiation. The progress of reaction was monitored by TLC and LCMS. The reaction mixture was filtered through celite and washed with CH_2Cl_2. The filtrate was concentrated under reduced pressure and purified by Combi-flash column chromatography. Pure fractions were concentrated under reduced pressure to obtain the desired compound (9.5-30%).

General procedure 42-43: To the stirred solution of 5-chloro-2-(6-methylpyridazin-4-yl)thieno[3,2-b]pyridine **37** (1 eq) and the respective amine (1.2 eq) in toluene (3 mL) was added sodium *tert*-butoxide (3 eq). The reaction mixture was purged for 10 min with argon gas. BINAP (0.15 eq) and $Pd_2(dba)_3$ (0.1 eq) were added at room temperature and the reaction mixture was stirred at 100 °C for 40 min under microwave irradiation. The progress of reaction was monitored by TLC and LCMS. The reaction mixture was filtered through celite and washed with CH_2Cl_2. The filtrate was concentrated under reduced pressure and purified by Combi-flash column chromatography. Pure fractions were concentrated under reduced pressure to obtain the desired compound (8.5-33%).

General procedure 45-48: To a stirred solution of 5-chloro-2-(pyridin-3-yl)thieno[3,2-b]pyridine **44** (100 mg, 1 eq) and the respective amine (hydrochloride) (7 eq) in DMSO (0.1-3 mL) was added K_2CO_3 (10 eq). The resulting reaction mixture was heated at 140 °C for 18 h to 4 days. The progress of the reaction was monitored by TLC and LCMS. After completion, the reaction mixture was cooled to RT, quenched with water (20 mL), extracted with 5% MeOH in DCM (2 x 30 mL) and washed with water. The organic layer was dried over Na_2SO_4, concentrated *in vacuo* and purified by preparative HPLC to afford the product (6-29%).

General procedure 50-55, Asyn-44: The synthesis was performed according to a literature procedure.[17] In brief, to a microwave tube were added compound **49** (1 eq), the respective

10.1002/chem.202303921

nitrogen nucleophile (5 eq), *n*-BuOH, followed by *N,N'*-diisopropylethylamine (7 eq). The tube was sealed and heated at 200 °C for 1 hour using a microwave reactor. The solvent was removed under reduced pressure and the residue was taken up in dichloromethane, washed with ammonium chloride saturated solution and water, dried over Na_2SO_4, and concentrated under reduced pressure. The residue was purified by flash column chromatography to afford the desired product.

4. ^{1}H NMR (400 MHz, DMSO-d_6) δ = 9.11 (s, 1H), 8.87 - 8.80 (m, 1H), 8.72 - 8.66 (m, 2H), 8.53 (s, 1H), 8.14 (d, *J* = 8.3 Hz, 1H), 7.91 (d, *J* = 4.9 Hz, 1H), 7.72 - 7.68 (m, 1H), 7.42 -7.37 (m, 1H) ppm. LCMS: 96.73 %, 313.2 $[M+H]^+$. HPLC: 95.06 % purity (Column: X-Bridge C18 (4.6 x 150) mm 5 mm, Mobile Phase: A – 5 mM Ammonium Bicarbonate in water, B - Acetonitrile).

5. ^{1}H NMR (400 MHz, DMSO-d_6) δ = 9.11 (br s, 1H), 8.84 (d, *J* = 7.3 Hz, 1H), 8.69 (d, *J* = 8.8 Hz, 1H), 8.48 (br s, 1H), 8.14 (d, *J* = 8.3 Hz, 1H), 7.95 - 7.69 (m, 1H), 7.41 (d, *J* = 8.3 Hz, 2H) ppm. LCMS: 98.92 %, 297.2 $[M+H]^+$. HPLC: 98.90 % purity (Column: X-Bridge C18 (4.6 x 150) mm 5 mm, Mobile Phase: A - 5mM Ammonium Bicarbonate in water, B - Acetonitrile).

6. ^{1}H NMR (400 MHz, DMSO-d_6) δ = 9.94 (s, 1H), 9.09 (s, 1H), 8.99 (s, 1H), 8.79 (d, *J* = 8.8 Hz, 2H), 8.42 (s, 1H), 8.20 (d, *J* = 8.8 Hz, 1H), 7.44 - 7.41 (m, 1H), 2.74 (s, 3H) ppm. LCMS: 97.45 %, 323.2 $[M+H]^+$. HPLC: 92.46 % purity (Column: X-Bridge C18 (4.6 x 150) mm 3.5 mm, Mobile Phase: A - 5mM Ammonium Bicarbonate in water, B - Acetonitrile).

7. ^{1}H NMR (400 MHz, DMSO-d_6) δ = 10.06 (s, 1H), 9.38 (d, *J* = 5.4 Hz, 1H), 9.10 (s, 1H), 9.04 (s, 1H), 8.83 - 8.77 (m, 2H), 8.61 (d, *J* = 3.4 Hz, 1H), 8.20 (d, *J* = 8.8 Hz, 1H), 7.41 (d, *J* = 8.3 Hz, 1H) ppm. LCMS: 98.24 %, 309.2 $[M+H]^+$. HPLC: 99.41 % purity (Column: X-Select CSH C18 (4.6 x 150) mm 5 mm, Mobile Phase: A - 0.1% TFA in water, B - Acetonitrile).

8. ^{1}H NMR (400 MHz, DMSO-d_6) δ = 8.91 (s, 1H), 8.48 (d, *J* = 8.3 Hz, 1H), 8.31 (d, *J* = 8.8 Hz, 1H), 8.13 (d, *J* = 5.4 Hz, 1H), 7.88 (d, *J* = 8.3 Hz, 1H), 7.57 (d, *J* = 5.4 Hz, 1H), 7.02 (d, *J* = 8.8 Hz, 1H), 5.02 - 4.81 (m, 1H), 3.89 - 3.82 (m, 2H), 3.65 - 3.56 (m, 2H), 1.98 - 1.90 (m, 2H), 1.76 - 1.69 (m, 2H) ppm. LCMS: 99.76 %, 314.7 $[M+H]^+$. HPLC: 99.17 % purity (Mobile Phase: A - 5mM Ammonium Bicarbonate in water, B - Acetonitrile).

9. ^{1}H NMR (400 MHz, Choroform-d) δ = 8.84 (d, *J* = 2.1 Hz, 1H), 8.60 (d, *J* = 2.1 Hz, 1H), 8.27 - 8.21 (m, 1H), 7.79 (d, *J* = 5.5 Hz, 1H), 7.66 - 7.57 (m, 2H), 4.96 - 4.79 (m, 1H), 3.61 - 3.36 (m, 5H), 2.17 - 1.97 (m, 4H) ppm. LCMS: 93.85 %, 393.8 $[M+H]^+$. HPLC: 94.37% purity (Mobile Phase: A - 5mM Ammonium Bicarbonate in water, B - Acetonitrile).

10. ^{1}H NMR (400 MHz, DMSO-d_6) δ = 13.00 (br s, 1H), 8.95 (s, 1H), 8.67 - 8.52 (m, 2H), 8.17 (d, *J* = 5.5 Hz, 1H), 7.99 (d, *J* = 8.5 Hz, 1H), 7.82 (br s, 1H), 7.63 (d, *J* = 5.5 Hz, 1H), 6.76 (br s, 1H), 4.94 - 4.74 (m, 1H), 3.12 - 3.04 (m, 4H), 2.01 - 1.89 (m, 2H), 1.81 - 1.71 (m, 2H) ppm. LCMS: 95.21 %, 380.2 $[M+H]^+$. HPLC: 97.39 % purity (Column: X-Bridge C18 (4.6*150) mm 5u, Mobile Phase: A - 5mM Ammonium Bicarbonate in water, B - Acetonitrile).

11. ^{1}H NMR (400 MHz, DMSO-d_6) δ = 8.88 (d, *J* = 2.4 Hz, 1H), 8.56 (d, *J* = 8.3 Hz, 1H), 8.39 (d, *J* = 2.0 Hz, 1H), 8.26 (s, 1H), 8.17 (d, *J* = 5.4 Hz, 1H), 8.02 - 7.98 (m, 2H), 7.62 (d, *J* = 5.4 Hz, 1H), 4.94 - 4.75 (m, 1H), 3.92 (s, 3H), 3.26 (br s, 2H), 3.10 - 3.02 (m, 2H), 2.05 - 1.93 (m, 2H), 1.83 (d, *J* = 2.4 Hz, 2H) ppm. LCMS: 98.26 %, 394.2 $[M+H]^+$. HPLC: 95.06 % purity (Column: X-Bridge C18 (4.6*150) mm 5u, Mobile Phase: A - 5mM Ammonium Bicarbonate in water, B - Acetonitrile).

12. ^{1}H NMR (400 MHz, Chloroform-d) δ = 8.81 (d, *J* = 1.5 Hz, 1H), 8.32 (d, *J* = 1.5 Hz, 1H), 8.23 (d, *J* = 8.3 Hz, 1H), 7.76 (d, *J* = 5.4 Hz, 1H), 7.67 (d, *J* = 8.8 Hz, 1H), 7.60 - 7.57 (m, 2H), 7.50 (d, *J* = 4.9 Hz, 1H), 7.41 - 7.39 (m, 1H), 4.86 - 4.67 (m, 1H), 3.44 - 3.37 (m, 2H), 3.16 - 3.10 (m, 2H), 1.99 - 1.83 (m, 4H) ppm. LCMS: 95.89 %, 396.0 $[M+H]^+$. HPLC: 98.56 % purity (Column: X-Bridge C18 (4.6 x 150) mm 5 mm, Mobile Phase: A - 5mM Ammonium bicarbonate in water, B - Acetonitrile).

13. ^{1}H NMR (400 MHz, DMSO-d_6) δ = 9.65 (d, *J* = 2.1 Hz, 1H), 8.94 (d, *J* = 2.3 Hz, 1H), 8.57 (d, *J* = 8.6 Hz, 1H), 8.50 (s, 1H), 8.36 - 8.29 (m, 1H), 8.01 - 7.93 (m, 2H), 7.04 (d, *J* = 9.1 Hz, 1H), 5.02 - 4.84 (m, 1H), 3.88 - 3.81 (m, 2H), 3.65 - 3.56 (m, 2H), 2.71 (s, 3H), 2.03 - 1.89 (m, 2H), 1.78 - 1.67 (m, 2H) ppm. LCMS: 96.91 %, 406.2 $[M+H]^+$. HPLC: 98.04% purity (Column: X Select CSH C18 (150 x 4.6) mm, 3.5 mm, Mobile phase A: 0.05% TFA; ACN (95:05), Mobile phase B: 0.05% TFA; ACN (05:95).

14. ^{1}H NMR (400 MHz, DMSO-d_6) δ = 9.33 (s, 2H), 9.24 (s, 1H), 8.90 (s, 1H), 8.38 – 8.36 (m, 1H), 8.32 (s, 1H), 7.95 – 7.96 (m, 1H), 7.99 (d, *J* = 8.7 Hz, 1H), 7.04 (d, *J* = 8.9 Hz, 1H), 5.03 - 4.85 (m, 1H), 3.89 - 3.81 (m, 2H), 3.65 - 3.57 (m, 2H), 2.02 - 1.89 (m, 2H), 1.78 - 1.67 (m, 2H) ppm. LCMS: 94.53%, 391.9 $[M+H]^+$. HPLC: 92.77% purity (Column: X Select CSH C18 (150 x4.6) mm, 3.5µ, Mobile phase A: 0.1% FA in Water: ACN (95:05), Mobile phase B: Acetonitrile).

15. ^{1}H NMR (400 MHz, DMSO-d_6) δ = 9.84 - 9.81 (m, 1H), 9.36 – 9.31 (m, 1H), 8.95 (d, *J* = 2.3 Hz, 1H), 8.61 - 8.54 (m, 2H), 8.35 - 8.31 (m, 1H), 8.11 – 8.08 (m, 1H), 7.99 (d, *J* = 8.7 Hz, 1H), 7.04 (d, *J* = 8.9 Hz, 1H), 5.03 - 4.85 (m, 1H), 3.89 - 3.81 (m, 2H), 3.65 - 3.57 (m, 2H), 2.02 - 1.89 (m, 2H), 1.78 - 1.67 (m, 2H) ppm. LCMS: 98.64 %, 392.0 $[M+H]^+$. HPLC: 99.69% purity (Column: X Select CSH C18 (150 x 4.6) mm, 3.5 mm, Mobile phase A: 0.1% FA in Water: ACN (95:05), Mobile phase B: Acetonitrile).

16. ^{1}H NMR (400 MHz, DMSO-d_6) δ ppm 1.73 (dtd, *J* = 10.08, 6.65, 6.65, 3.63 Hz, 2 H) 1.87 - 2.00 (m, 2 H) 2.56 (s, 3 H) 3.56 - 3.64 (m, 2 H) 3.81 - 3.89 (m, 2 H) 4.80 - 5.05 (m, 1 H) 7.04 (d, *J* = 9.01 Hz, 1 H) 7.67 (dd, *J* = 5.25, 1.38 Hz, 1 H) 7.74 (s, 1 H) 7.94 (d, *J* = 8.63 Hz, 1 H) 8.31 (s, 1 H) 8.33 (d, *J* = 2.50 Hz, 1 H) 8.50 - 8.58 (m, 2 H) 8.94 (d, *J* = 2.38 Hz, 1 H). LCMS: 97.22 %, 405.4 $(M+H)^+$. HPLC: 98.4% purity (Method: - HPLC_X-Select, Column : X-Select CHS C18 (4.6 x 150) mm 5 mm, Mobile Phase: A - 0.1% FA in (ACN:Water)(50:950) B – Acetonitrile).

17. ^{1}H NMR (400 MHz, DMSO-d_6) δ ppm 1.73 (ddd, *J* = 9.90, 6.54, 3.00 Hz, 2 H) 1.90 - 1.99 (m, 2 H) 3.57 - 3.63 (m, 2 H) 3.82 - 3.88 (m, 2 H) 4.84 - 5.02 (m, 1 H) 7.04 (d, *J* = 9.29 Hz, 1 H) 7.86 - 7.89 (m, 2 H) 7.95 (d, *J* = 8.68 Hz, 1 H) 8.32 (dd, *J* = 8.99, 2.51 Hz, 1 H) 8.35 (s, 1 H) 8.54 (d, *J* = 8.68 Hz, 1 H) 8.69 - 8.71 (m, 2 H) 8.94 (d, *J* = 2.08 Hz, 1 H). LCMS: 98.4 %, 391.0 $(M+H)^+$. HPLC: 99.6 % purity (Column: X select C18 5um (4.6 x 150 mm), Mobile Phase: A: 5 mM Ammonium Acetate in Water, Mobile Phase: B: 100% ACN).

18. ^{1}H NMR (400 MHz, DMSO-d_6) δ ppm 1.69 - 1.76 (m, 2 H) 1.90 - 1.99 (m, 2 H) 3.57 - 3.63 (m, 2 H) 3.82 - 3.87 (m, 2 H) 4.85 - 5.01 (m, 1 H) 7.03 (d, *J* = 8.93 Hz, 1 H) 7.46 (d, *J* = 7.21 Hz, 1 H) 7.50

- 7.54 (m, 2 H) 7.86 - 7.90 (m, 3 H) 8.04 (s, 1 H) 8.32 (dd, *J* = 8.99, 2.51 Hz, 1 H) 8.46 (d, *J* = 8.56 Hz, 1 H) 8.92 (d, *J* = 2.20 Hz, 1 H). LCMS: 97.1 %, 390.2 $(M+H)^+$. HPLC: 97.4 % purity (Column: X select C18 5um (4.6 x 150mm), Mobile Phase: A: 5Mm Ammonium Acetate in Water, Mobile Phase: B : 100% ACN).

19. ^{1}H NMR (400 MHz, DMSO-d_6) δ ppm 1.68 - 1.78 (m, 2 H) 1.89 - 2.01 (m, 2 H) 2.40 (s, 3 H) 3.57 - 3.64 (m, 2 H) 3.81 - 3.89 (m, 2 H) 4.83 - 5.02 (m, 1 H) 7.03 (br d, *J* = 9.05 Hz, 1 H) 7.90 (d, *J* = 8.56 Hz, 1 H) 8.10 (br s, 1 H) 8.15 (s, 1 H) 8.32 (dd, *J* = 8.62, 1.65 Hz, 1 H) 8.46 - 8.52 (m, 2 H) 8.92 (d, *J* = 2.57 Hz, 2 H). LCMS: 97.5 %, 405.1 $(M+H)^+$. HPLC: 98.3% purity (Column: X select C18 5um (4.6 x 150mm), Mobile Phase: A: 5Mm Ammonium Acetate in Water, Mobile Phase: B: 100% ACN).

20. ^{1}H NMR (400 MHz, DMSO-d_6) δ = 9.05 (s, 1H), 8.57 (d, *J* = 8.8 Hz, 1H), 8.40 (br s, 1H), 8.35 (d, *J* = 4.9 Hz, 1H), 8.17 (d, *J* = 4.9 Hz, 1H), 8.05 (d, *J* = 8.3 Hz, 1H), 7.73 (d, *J* = 3.4 Hz, 1H), 7.62 (d, *J* = 5.4 Hz, 1H), 7.56 (s, 1H), 4.92 - 4.74 (m, 1H), 3.30 - 3.26 (m, 2H), 3.11 (br s, 2H), 1.96 - 1.80 (m, 2H), 1.69 (br s, 2H) ppm. LCMS: 99.59 %, 409.2 $[M+H]^+$. HPLC: 96.93 % purity (Column: X-Bridge C18 (4.6*150) mm 5u, Mobile Phase: A - 5mM Ammonium Bicarbonate in water, B - Acetonitrile).

21. ^{1}H NMR (400 MHz, DMSO-d_6) δ = 9.05 (br s, 1H), 8.55 (d, *J* = 8.3 Hz, 1H), 8.37 (s, 1H), 8.33 - 8.29 (m, 1H), 8.25 (t, *J* = 8.3 Hz, 1H), 8.17 (d, *J* = 4.9 Hz, 1H), 8.01 (d, *J* = 8.8 Hz, 1H), 7.64 - 7.56 (m, 1H), 7.53 (s, 1H), 4.87 - 4.69 (m, 1H), 3.27 (br s, 2H), 3.07 (s, 2H), 1.85 - 1.71 (m, 2H), 1.59 (s, 2H) ppm. LCMS: 99.59 %, 409.2 $[M+H]^+$. HPLC: 96.93 % purity (Column: X-Bridge C18 (4.6*150) mm 5u, Mobile Phase: A - 5mM Ammonium Bicarbonate in water, B - Acetonitrile).

22. ^{1}H NMR (400 MHz, DMSO-d_6) δ ppm 1.71 - 1.77 (m, 2 H) 1.91 - 1.99 (m, 2 H) 3.58 - 3.64 (m, 2 H) 3.83 - 3.88 (m, 2 H) 4.82 - 5.03 (m, 1 H) 7.05 (d, *J* = 9.26 Hz, 1 H) 7.68 - 7.72 (m, 1 H) 7.81 - 7.85 (m, 1 H) 7.93 (d, *J* = 8.63 Hz, 1 H) 8.08 (d, *J* = 8.63 Hz, 1 H) 8.14 (d, *J* = 7.63 Hz, 1 H) 8.33 (d, *J* = 2.50 Hz, 1 H) 8.36 (s, 1 H) 8.54 (d, *J* = 8.63 Hz, 1 H) 8.81 (d, *J* = 2.13 Hz, 1 H) 8.95 (d, *J* = 2.25 Hz, 1 H) 9.51 (d, *J* = 2.38 Hz, 1 H). LCMS: 99.4 %, 441.4 $(M+H)^+$. HPLC: 97.4 % purity (Column: X-Select CSH C18 (4.6 x 150) mm 5 mm, Mobile Phase: A - 0.1% Formic acid in water : Acetonitrile (95:05), B – Acetonitrile)

23. ^{1}H NMR (400 MHz, DMSO-d_6) δ ppm 1.73 (ddt, *J* = 13.22, 6.65, 3.33, 3.33 Hz, 2 H) 1.85 - 2.03 (m, 2 H) 3.56 - 3.64 (m, 2 H) 3.80 - 3.86 (m, 2 H) 3.87 (s, 3 H) 4.84 - 5.02 (m, 1 H) 7.00 - 7.05 (m, 2 H) 7.43 (d, *J* = 5.50 Hz, 3 H) 7.87 (d, *J* = 8.68 Hz, 1 H) 8.09 (s, 1 H) 8.31 (dd, *J* = 8.99, 2.51 Hz, 1 H) 8.45 (d, *J* = 8.56 Hz, 1 H) 8.92 (d, *J* = 2.32 Hz, 1 H). LCMS: 99.2 %, 420.4 $(M+H)^+$. HPLC: 99.0% purity(Column: X select C18 5 mm (4.6 x 150 mm), Mobile Phase: A: 5 mM Ammonium Acetate in Water Mobile Phase: B: 100% ACN)

24. ^{1}H NMR (400 MHz, Chloroform-d) δ = 8.69 (d, *J* = 2.3 Hz, 1H), 8.21 (d, *J* = 8.6 Hz, 1H), 7.89 (d, *J* = 2.3 Hz, 1H), 7.76 (d, *J* = 5.5 Hz, 1H), 7.66 - 7.58 (m, 2H), 4.94 - 4.76 (m, 1H), 3.64 - 3.56 (m, 2H), 3.35 - 3.28 (m, 2H), 2.14 - 1.95 (m, 5H), 1.12 - 1.06 (m, 2H), 0.93 - 0.87 (m, 2H) ppm. LCMS: 99.34 %, 354.2 $[M+H]^+$. HPLC: 98.15 % purity (Column: X-Bridge C18 (4.6 x 150) mm 5 mm, Mobile Phase: A - 5mM Ammonium bicarbonate in water, B - Acetonitrile).

25. ^{1}H NMR (400 MHz, Chloroform-d) δ = 8.76 (d, *J* = 2.4 Hz, 1H), 8.22 (d, *J* = 8.5 Hz, 1H), 8.15 (d, *J* = 2.4 Hz, 1H), 7.76 (d, *J* = 5.5 Hz, 1H), 7.65 (d, *J* = 8.5 Hz, 1H), 7.60 (d, *J* = 5.5 Hz, 1H), 5.31 - 5.28 (m, 1H), 5.22 - 5.17 (m, 1H), 4.92 - 4.73 (m, 1H), 3.69 - 3.59 (m, 2H), 3.43 - 3.33 (m, 2H), 2.15 (s, 3H), 2.10 - 1.88 (m, 4H) ppm. LCMS: 99.61 %, 354.2 $[M+H]^+$. HPLC: 99.78 % purity (Column: X-Bridge C18 (4.6 x 150) mm 5 mm, Mobile Phase: A – 5 mM Ammonium Bicarbonate in water, B - Acetonitrile).

26. ^{1}H NMR (400 MHz, methanol-d_4) δ ppm 1.84 (ddd, *J* = 13.57, 6.88, 3.44 Hz, 2 H) 1.95 - 2.03 (m, 2 H) 3.33 - 3.36 (m, 1 H) 3.48 (dt, *J* = 3.25, 1.63 Hz, 1 H) 3.63 (ddd, *J* = 13.35, 6.85, 4.06 Hz, 3 H) 3.83 (d, *J* = 2.63 Hz, 1 H) 4.62 - 4.67 (m, 2 H) 5.03 (t, *J* = 6.75 Hz, 2 H) 5.49 (s, 1 H) 6.09 (s, 1 H) 6.95 (d, *J* = 8.50 Hz, 1 H) 7.32 (d, *J* = 8.25 Hz, 1 H) 7.94 (dd, *J* = 8.25, 0.63 Hz, 1 H) 8.09 (dd, *J* = 8.94, 2.56 Hz, 1 H) 8.64 - 8.67 (m, 1 H). LCMS: 96.1 %, 385.2 $(M+H)^+$. HPLC: 98.3% purity (Column: ACE Excel 2 C18-AR,100 mm x 3.0 mm, Mobile Phase A: 0.05% TFA in Water, Mobile Phase B: 0.05% TFA in Acetonitrile).

27. ^{1}H NMR (400 MHz, DMSO-d_6) δ ppm 1.40 - 1.50 (m, 2 H) 1.66 - 1.75 (m, 3 H) 1.98 (d, *J* = 11.76 Hz, 3 H) 3.17 (s, 1 H) 3.44 (d, *J* = 2.00 Hz, 3 H) 3.52 - 3.57 (m, 3 H) 3.84 - 3.91 (m, 3 H) 6.96 (d, *J* = 9.13 Hz, 1 H) 7.18 (d, *J* = 7.63 Hz, 1 H) 7.37 (d, *J* = 8.25 Hz, 1 H) 7.93 (d, *J* = 8.13 Hz, 1 H) 8.19 (dd, *J* = 8.88, 2.50 Hz, 1 H) 8.29 (s, 1 H) 8.80 (d, *J* = 2.25 Hz, 1 H). LCMS: 90.4 %, 411.0 $(M-H)^+$. HPLC: 95.1 % purity (Column: ACE Excel 2 C18-AR, 100 mm x 3.0 mm, Mobile Phase A: 0.05% TFA in Water, Mobile Phase B: 0.05% TFA in Acetonitrile).

28. ^{1}H NMR (400 MHz, DMSO-d_6) δ ppm 1.66 - 1.78 (m, 2 H) 1.85 - 2.00 (m, 2 H) 3.50 - 3.58 (m, 2 H) 3.75 - 3.86 (m, 2 H) 4.70 - 5.04 (m, 1 H) 6.26 (s, 1 H) 6.90 (dd, *J* = 6.19, 3.06 Hz, 1 H) 6.95 (d, *J* = 9.13 Hz, 1 H) 7.24 (d, *J* = 8.00 Hz, 1 H) 7.73 (d, *J* = 8.00 Hz, 1 H) 8.20 (dd, *J* = 9.01, 2.50 Hz, 1 H) 8.26 (d, *J* = 6.13 Hz, 1 H) 8.36 (d, *J* = 2.38 Hz, 1 H) 8.75 - 8.80 (m, 1 H). LCMS: 97.0 %, 407.22 $(M+H)^+$. HPLC: 91.4 % purity (Method- HPLC_X-Select(TFA) Column : X-Select CSH C18 (4.6 x 150) mm 5 mm, Mobile Phase: A - 0.1% TFA in water, B – Acetonitrile).

29. ^{1}H NMR (400 MHz, Chloroform-d) δ = 9.00 (d, *J* = 2.5 Hz, 1H), 8.58 (d, *J* = 2.5 Hz, 1H), 8.25 (d, *J* = 8.5 Hz, 1H), 7.80 (d, *J* = 5.5 Hz, 1H), 7.62 - 7.57 (m, 2H), 5.03 - 4.97 (m, 1H), 4.91 - 4.86 (m, 1H), 4.00 - 3.91 (m, 2H), 3.91 - 3.80 (m, 2H), 2.14 - 2.00 (m, 4H) ppm. LCMS: 100 %, 338.9 $[M+H]^+$. HPLC: 99.83 % purity (Column : X-Bridge C18 (4.6 x150) mm 5 mm, Mobile Phase: A - 5mM Ammonium bicarbonate in water, B - Acetonitrile).

30. ^{1}H NMR (400 MHz, DMSO-d_6) δ = 9.04 (t, *J* = 2.4 Hz, 1H), 8.68 (t, *J* = 2.2 Hz, 1H), 8.56 - 8.52 (m, 1H), 8.19 - 8.15 (m, 1H), 7.98 – 7.94 (m, 1H), 7.64 – 7.61 (m, 1H), 5.02 - 4.83 (m, 1H), 4.38 - 4.29 (q, 2H), 3.62 - 3.52 (m, 2H), 3.42 - 3.34 (m, 2H), 2.06 - 1.91 (m, 2H), 1.84 - 1.73 (m, 2H), 1.38 - 1.32 (t, 3H) ppm. LCMS: 88.38 %, 386.6 $[M+H]^+$. HPLC: 88.20 % purity (Column: X-Select CSH C18 (4.6 x 150) mm 5 mm, Mobile Phase: A - 0.1% TFA in water, B - Acetonitrile).

31. ^{1}H NMR (400 MHz, DMSO-d_6) δ = 13.21 (br s, 1H), 9.02 (d, *J* = 2.5 Hz, 1H), 8.72 (d, *J* = 2.4 Hz, 1H), 8.53 (d, *J* = 8.5 Hz, 1H), 8.16 (d, *J* = 5.5 Hz, 1H), 7.96 (d, *J* = 8.6 Hz, 1H), 7.64 - 7.61 (m, 1H), 5.02 - 4.84 (m, 1H), 3.64 - 3.56 (m, 2H), 3.47 - 3.39 (m, 2H), 2.07 - 1.92 (m, 2H), 1.85 - 1.74 (m, 2H) ppm. LCMS: 91.62 %, 358.0 [M+H]+. HPLC: 93.67% purity (Column: X-Select CSH C18

(4.6 x 150) mm 5 mm, Mobile Phase: A - 0.1% Formic acid in water: Acetonitrile (95:5), B - Acetonitrile).

32. ^{1}H NMR (400 MHz, DMSO-d_6) δ = 8.99 (d, *J* = 2.5 Hz, 1H), 8.55 – 8.51 (m, 1H), 8.26 (d, *J* = 2.5 Hz, 1H), 8.16 (d, *J* = 5.5 Hz, 1H), 7.97 (d, *J* = 8.6 Hz, 1H), 7.60 (dd, *J* = 0.6, 5.5 Hz, 1H), 4.98 - 4.81 (m, 1H), 3.57 (br s, 2H), 3.42 - 3.34 (m, 2H), 3.04 (s, 3H), 2.88 (s, 3H), 2.03 - 1.89 (m, 2H), 1.82 - 1.71 (m, 2H) ppm. LCMS: 99.47 %, 385.2 [M+H]+. HPLC: 98.36 % purity (Column: X-Select CSH C18 (4.6 x 150) mm 5 mm, Mobile Phase: A - 0.1% TFA in water, B - Acetonitrile).

33. ^{1}H NMR (400 MHz, DMSO-d_6) δ = 8.98 (d, *J* = 2.4 Hz, 1H), 8.53 (d, *J* = 9.1 Hz, 1H), 8.46 - 8.39 (m, 2H), 8.16 (d, *J* = 5.5 Hz, 1H), 7.96 (d, *J* = 8.6 Hz, 1H), 7.63 - 7.59 (m, 1H), 4.99 - 4.81 (m, 1H), 3.61 - 3.48 (m, 2H), 3.37 - 3.31 (m, 2H), 2.81 (d, *J* = 4.8 Hz, 3H), 2.03 - 1.92 (m, 2H), 1.84 - 1.74 (m, 2H) ppm. LCMS: 99.07 %, 371.4 $[M+H]^+$. HPLC: 99.78 % purity (Column: X-Select CSH C18 (4.6 x 150) mm 5 mm, Mobile Phase: A - 0.1% Formic acid in water: Acetonitrile (95:5), B - Acetonitrile).

34. ^{1}H NMR (400 MHz, DMSO-d_6) δ = 8.89 (d, *J* = 2.5 Hz, 1H), 8.58 - 8.53 (m, 2H), 8.17 (d, *J* = 5.5 Hz, 1H), 7.95 (d, *J* = 8.6 Hz, 1H), 7.65 - 7.61 (m, 1H), 5.43 (t, *J* = 5.6 Hz, 1H), 4.97 - 4.78 (m, 1H), 4.55 (d, *J* = 5.5 Hz, 2H), 3.39 - 3.34 (m, 2H), 3.18 - 3.09 (m, 2H), 2.07 - 1.96 (m, 2H), 1.90 - 1.81 (m, 2H) ppm. LCMS: 93.06 %, 344.1 $[M+H]^+$. HPLC: 96.41 % purity (Column: X-Select CSH C18 (4.6 x 150) mm 5 mm, Mobile Phase: A - 0.1% Formic acid in water: Acetonitrile (95:5), B - Acetonitrile).

35. ^{1}H NMR (400 MHz, DMSO-d_6) δ = 8.94 (d, *J* = 2.4 Hz, 1H), 8.54 (d, *J* = 8.6 Hz, 1H), 8.47 (d, *J* = 2.4 Hz, 1H), 8.17 (d, *J* = 5.5 Hz, 1H), 7.96 (d, *J* = 8.5 Hz, 1H), 7.63 (d, *J* = 5.5 Hz, 1H), 4.97 - 4.79 (m, 1H), 4.47 (s, 2H), 3.42 - 3.35 (m, 5H), 3.21 - 3.13 (m, 2H), 2.14 - 1.95 (m, 2H), 1.95 - 1.80 (m, 2H) ppm. LCMS: 98.12 %, 358.4 $[M+H]^+$. HPLC: 97.14 % purity (Column: X-Select CSH C18 (4.6 x 150) mm 5 mm, Mobile Phase: A - 0.1% Formic acid in water: Acetonitrile (95:5), B - Acetonitrile).

38. ^{1}H NMR (400 MHz, DMSO-d_6) δ ppm 1.78 (ddd, *J* = 10.29, 6.72, 3.50 Hz, 2 H) 1.93 - 2.03 (m, 2 H) 2.72 (s, 3 H) 3.35 (br d, *J* = 3.38 Hz, 2 H) 3.49 - 3.58 (m, 2 H) 4.81 - 4.99 (m, 1 H) 6.91 (dd, *J* = 15.70, 2.19 Hz, 1 H) 6.97 (dd, *J* = 8.88, 2.38 Hz, 1 H) 7.78 (dd, *J* = 8.57, 1.56 Hz, 1 H) 7.91 - 7.98 (m, 2 H) 8.52 (s, 1 H) 8.58 (d, *J* = 8.75 Hz, 1 H) 9.66 (d, *J* = 2.00 Hz, 1 H). LCMS: 92.05 %, 423.2 $(M+H)^+$.

39. ^{1}H NMR (400 MHz, DMSO-d_6) δ ppm 1.75 - 1.86 (m, 2 H) 1.94 - 2.07 (m, 2 H) 2.71 (s, 3 H) 3.24 - 3.29 (m, 2 H) 3.48 - 3.56 (m, 2 H) 3.87 (s, 3 H) 4.79 - 4.99 (m, 1 H) 6.66 - 6.73 (m, 2 H) 7.77 (d, *J* = 8.63 Hz, 1 H) 7.90 (d, *J* = 8.63 Hz, 1 H) 7.95 (d, *J* = 2.13 Hz, 1 H) 8.44 - 8.51 (m, 2 H) 9.65 (d, *J* = 2.13 Hz, 1 H). LCMS: 95.1 %, 435.4 $(M+H)^+$. HPLC: 91.1 % purity (Column: X-Select CSH C18 (4.6 x 150) mm 5 mm, Mobile Phase: A - 0.1% Formic acid in water : Acetonitrile(95:05) B – Acetonitrile).

40. ^{1}H NMR (400 MHz, DMSO-d_6) δ ppm 1.75 (ddd, *J* = 13.63, 6.69, 3.31 Hz, 2 H) 1.95 (tdd, *J* = 16.96, 16.96, 8.29, 3.94 Hz, 2 H) 2.71 (s, 3 H) 3.81 - 3.90 (m, 2 H) 3.98 - 4.05 (m, 2 H) 4.87 - 5.05 (m, 1 H) 7.97 - 8.01 (m, 2 H) 8.53 (s, 1 H) 8.63 (d, *J*=8.63 Hz, 1 H) 9.15 (s, 2 H) 9.66 (d, *J* = 2.25 Hz, 1 H). LCMS: 99.6 %, 407.3 $(M+H)^+$. HPLC: 98.9 % purity (Column: X-Select CSH C18 (4.6 x 150) mm 5 mm, Mobile Phase: A - 0.1% Formic acid in water: Acetonitrile (95:05),B – Acetonitrile).

41. ^{1}H NMR (400 MHz, DMSO-d_6) δ ppm 2.73 (s, 3 H) 7.93 (s, 1 H) 8.01 (d, *J* = 2.25 Hz, 1 H) 8.16 (dt, *J* = 5.22, 1.58 Hz, 1 H) 8.26 (d, *J* = 8.63 Hz, 1 H) 8.43 (d, *J* = 5.25 Hz, 1 H) 8.61 (s, 1 H) 8.80 (d, *J* = 8.63 Hz, 1 H) 9.69 (d, *J* = 2.13 Hz, 1 H). LCMS: 98.6 %, 323.3 $(M+H)^+$. HPLC: 99.5 % purity (Column: X-Select CSH C18 (4.6 x 150) mm 5 mm. Mobile Phase: A - 0.1% Formic acid in water: Acetonitrile (95:05) B – Acetonitrile).

42. ^{1}H NMR (400 MHz, DMSO-d_6) δ ppm 1.65 (br dd, *J* = 12.44, 3.81 Hz, 2 H) 1.87 (d, *J* = 11.38 Hz, 2 H) 2.69 (s, 3 H) 2.86 (ddd, *J* = 12.04, 8.60, 3.25 Hz, 1 H) 2.95 - 3.02 (m, 2 H) 4.57 (d, *J* = 13.13 Hz, 2 H) 7.09 - 7.15 (m, 3 H) 7.31 (dd, *J* = 8.57, 5.57 Hz, 2 H) 7.87 (d, *J* = 2.25 Hz, 1 H) 8.18 - 8.24 (m, 2 H) 9.56 (d, *J* = 2.13 Hz, 1 H). LCMS: 91.6 %, 405.2 $(M+H)^+$. HPLC: 92.9 % purity (Method:- HPLC_X-Select(TFA) Column : X-Select CSH C18 (4.6 x 150) mm 5 mm Mobile Phase: A - 0.1% TFA in water, B – Acetonitrile).

43. ^{1}H NMR (400 MHz, DMSO-d_6) δ ppm 1.44 (q, *J* = 10.76 Hz, 2 H) 1.67 (br s, 2 H) 1.82 (d, *J* = 12.72 Hz, 2 H) 2.67 (br s, 3 H) 2.86 (t, *J* = 12.47 Hz, 2 H) 3.16 - 3.71 (m, 7 H) 4.43 (d, *J* = 11.74 Hz, 2 H) 4.57 - 4.72 (m, 1 H) 7.05 - 7.12 (m, 1 H) 7.85 (br s, 1 H) 8.16 (dd, *J* = 5.87, 1.47 Hz, 3 H) 9.55 (br s, 1 H). LCMS: 99.4 %, 412 $(M+H)^+$. HPLC: 95.0 % purity (Method:- HPLC_X-Bridge, Column : X-Bridge C18 (4.6 x 150) mm 5.0 µm Mobile Phase: A - 5 mM ABC in Water, B – Acetonitrile).

45. ^{1}H NMR (400 MHz, DMSO-d_6) δ = 9.30 (s, 1H), 8.54 (d, *J* = 4.4 Hz, 1H), 8.47 (d, *J* = 8.3 Hz, 1H), 8.37 (s, 1H), 8.24 (d, *J* = 9.3 Hz, 1H), 7.53 - 7.48 (m, 1H), 7.13 (d, *J* = 8.8 Hz, 1H), 5.01 - 4.82 (m, 1H), 3.88 – 3.80 (m, 2H), 3.61 - 3.53 (m, 2H), 2.04 - 1.91 (m, 2H), 1.80 - 1.70 (m, 2H) ppm. LCMS: 96.52 %, 314.2 $[M+H]^+$. HPLC: 83.90 % purity (Column: X-Bridge C18 (4.6 x 150) mm 5 mm, Mobile Phase: A - 5mM Ammonium Bicarbonate in water, B - Acetonitrile).

46. ^{1}H NMR (400 MHz, Chloroform-d) δ = 9.36 (s, 1H), 8.57 (d, *J* = 3.9 Hz, 1H), 8.46 (d, *J* = 7.8 Hz, 1H), 7.95 (d, *J* = 8.8 Hz, 1H), 7.81 (s, 1H), 7.41 - 7.35 (m, 1H), 6.56 (d, *J* = 8.8 Hz, 1H), 5.52 - 5.27 (m, 1H), 4.04 - 3.86 (m, 1H), 3.83 - 3.64 (m, 3H), 2.51 - 2.32 (m, 1H), 2.28 - 2.09 (m, 1H) ppm. LCMS: 99.65 %, 300.1 $[M+H]^+$. HPLC: 99.51 % purity (Column: X-Bridge C18 (4.6 x 150) mm 5 mm, Mobile Phase: A - 5mM Ammonium Bicarbonate in water, B - Acetonitrile).

47. ^{1}H NMR (400 MHz, Chloroform-d) δ = 9.30 (s, 1H), 8.60 (d, *J* = 3.9 Hz, 1H), 8.34 (d, *J* = 7.3 Hz, 1H), 8.02 (d, *J* = 9.3 Hz, 1H), 7.83 (s, 1H), 7.43 - 7.37 (m, 1H), 6.83 (d, *J* = 9.3 Hz, 1H), 3.89 - 3.86 (m, 4H), 3.64 - 3.61 (m, 4H) ppm. LCMS: 98.25 %, 298.1 $[M+H]^+$. HPLC: 99.43 % purity (Column: X-Bridge C18 (4.6 x 150) mm 5 mm, Mobile Phase: A - 5mM Ammonium Bicarbonate in water, B - Acetonitrile).

48. ^{1}H NMR (400 MHz, DMSO-d_6) δ = 9.30 (d, *J* = 1.8 Hz, 1H), 8.54 (s, 1H), 8.51 – 8.44 (m, 1H), 8.37 (s, 1H), 8.24 (d, *J* = 9.0 Hz, 1H), 7.52 - 7.48 (m, 1H), 7.07 (d, *J* = 9.1 Hz, 1H), 3.61 - 3.56 (m, 4H), 2.48 - 2.42 (m, 4H), 2.23 (s, 3H) ppm. LCMS: 99.13 %, 311.2 $[M+H]^+$. HPLC: 95.21 % purity (Column: X-Bridge C18 (4.6 x 150) mm 5 mm, Mobile Phase: A – 5 mM Ammonium Bicarbonate in water, B - Acetonitrile).

50. ^{1}H NMR (400 MHz, DMSO-d_6) δ = 9.15 (s, 1H), 8.83 (s, 1H), 8.67 – 8.66 (m, 1H), 8.59 (d, *J* = 8.7 Hz, 1H), 8.54 (d, *J* = 8.4 Hz, 1H), 8.35 – 8.33 (m, 1H), 8.32 (s, 1H), 8.00 – 7.98 (d, *J* = 8.9 Hz,

1H), 7.59 – 7.62 (m, 1H), 6.83 (d, *J* = 8.9 Hz, 1H), 5.63 – 5.49 (m, 1H), 4.53 – 4.46 (m, 2H), 4.30 – 4.21 (m, 2H) ppm. LCMS: 94.53 %, 391.9 $[M+H]^+$. HPLC: 92.77 % purity (Column: X Select CSH C18 (150 x 4.6) mm, 3.5 mm, Mobile phase A: 0.1% FA in Water: ACN (95:05), Mobile phase B: Acetonitrile).

51. ^{1}H NMR (400 MHz, $CDCl_3$) δ = 9.05 (s, 1H), 8.82 – 8.79 (m, 1H), 8.62 – 8.58 (m, 1H), 8.38 – 7.96 (m, 3H), 7.82 (s, 1H), 7.62 – 7.53 (m, 1H), 7.47 – 7.40 (m, 1H), 6.51 – 6.49 (m, 1H), 5.61 – 5.45 (m, 1H), 4.25 – 4.11 (m, 4H).

52. ^{1}H NMR (400 MHz, $CDCl_3$) δ = 9.00 (s, 1H), 8.86 – 8.84 (m, 1H), 8.60 – 8.58 (m, 1H), 8.28 – 7.95 (m, 3H), 7.80 (s, 1H), 7.58 – 7.54 (m, 1H), 7.42 – 7.35 (m, 1H), 6.50 – 6.48 (m, 1H), 4.12 – 4.07 (m, 1H), 4.64 – 4.51 (m, 4H), 3.43 (s, 3H), 2.26 – 2.10 (m, 2H).

53. ^{1}H NMR (400 MHz, $CDCl_3$) δ = 9.01 (s, 1H), 8.86 – 8.84 (m, 1H), 8.62 – 8.60 (m, 1H), 8.30 – 7.96 (m, 3H), 7.81 (s, 1H), 7.59 – 7.53 (m, 1H), 7.43 – 7.36 (m, 1H), 6.51 – 6.49 (m, 1H), 4.13 – 4.08 (m, 1H), 4.65 – 4.52 (m, 4H), 3.42 (s, 3H), 2.28 – 2.08 (m, 2H).

54. ^{1}H NMR (400 MHz, $CDCl_3$) δ = 9.03 (s, 1H), 8.80 – 8.78 (m, 1H), 8.57 – 8.54 (m, 1H), 8.34 – 7.96 (m, 3H), 7.72 (s, 1H), 7.58 – 7.53 (m, 1H), 7.42 – 7.37 (m, 1H), 6.48 – 6.45 (m, 1H), 4.47 – 4.28 (m, 3H), 4.01 – 3.95 (m, 2H), 3.41 (s, 3H).

55. ^{1}H NMR (400 MHz, $CDCl_3$) δ = 9.02 (s, 1H), 8.86 – 8.84 (m, 1H), 8.60 – 8.57 (m, 1H), 8.32 – 7.97 (m, 3H), 7.76 (s, 1H), 7.62 – 7.54 (m, 1H), 7.46 – 7.38 (m, 1H), 6.74 – 6.72 (s, 1H), 4.95 – 4.73 (m, 1H), 3.82 – 3.68 (m, 4H), 2.04 – 1.85 (m, 4H).

Radiosynthesis of [^{18}F]asyn-44

The synthesis was carried out on a TRACERlab FX2 N radiosynthesis module. [^{18}F]Fluoride (5-20 GBq) was trapped on an anion exchange cartridge (HCO_3; Synthra, Germany) and was eluted with a solution of 1.35 mg K_2CO_3 and 14 mg Kryptofix® 222 in 0.9 mL MeOH and 0.1 mL water. It was azeotropically dried at 85-110 °C under addition of 1 mL MeCN with a N_2 flow and vacuum. The reaction vessel was then cooled to 60°C. The precursor (1 mg in 0.7 mL DMSO) was added, and the reaction mixture was stirred and heated at 100 °C. After 10 minutes, the reactor was cooled to 40 °C and the mixture was diluted with 4 mL mobile phase (MeCN/0.1M ammonium formate 45:55). The product was purified by semi-preparative HPLC (Luna C18 column (5 µm, 250 x 10 mm), MeCN/0.1M ammonium formate 45:55, 6 mL/min) and the fraction eluting at ~25 min was collected in a flask containing 25 mL water and passed over a C18 solid-phase extraction cartridge. The product was eluted with 1 mL ethanol, followed by 9 mL saline. [^{18}F]Asyn-44 was obtained in a total synthesis time of 1 hour with a radiochemical purity of >95%, a radiochemical yield of 6±2% (decay-corrected, n=5) and a molar activity of 263±121 GBq/µmol.

LogD$_{7.4}$ determination

The log$D_{7.4}$ of [^{18}F]asyn-44 was determined via the shake-flask method:[19] Briefly, 50 mL 1-octanol was added to a separatory funnel and washed three times with potassium phosphate buffer (50 mL, 0.025M, pH 7.4). Then, 100 µL of the formulated [^{18}F]asyn-44 solution was added to the 1-octanol phase and was washed twice more with the potassium phosphate buffer. Eight 3-mL aliquots were taken of the 1-octanol layer and added to test tubes containing 3 mL buffer solution. The tubes were shaken for 10 min and centrifuged (~3500-4000 rpm) for 5 min. Aliquots of the 1-octanol layers (0.5 mL each) and buffer layers (1.5 mL each) were taken, weighed and measured in a gamma counter (Perkin Elmer; Waltham, Massachusetts, US). The log$D_{7.4}$ was calculated by taking the natural logarithm of the ratio of counts per mL of the 1-octanol and corresponding buffer aliquots and was 4.16±0.04 (n=8).

Postmortem tissues

The binding assays utilized fresh frozen blocks (1 cm^3) of autopsy-confirmed human tissues at the University of Pittsburgh under the approval of the Committee for Oversight of Research and Clinical Training Involving Decedents (CORID). PD anterior cingulate cortex brain tissue was obtained from Dr. Thomas Beach at Banner/Sun Health Arizona, USA and contained frequent α-synuclein aggregates and no other detectable aggregated amyloid or TDP-43 species. AD and normal control brain tissues were obtained from the Neurodegenerative Disease Brain Bank at the University of California, San Francisco, USA and contained only frequent tau neurofibrillary tangles and Aβ plaque aggregates (AD tissue, middle frontal gyrus) and no other detectable aggregated amyloid or TDP-43 species (control tissue, middle frontal gyrus). The frozen tissue blocks were prepared for the binding assays as previously described.[21]

The autoradiography and IHC studies utilized post-mortem paraffin embedded tissue blocks from different brain regions of control donors and donors with confirmed α-syn and tau pathology, which were acquired from the University of Pennsylvania Brain Bank. The presence or absence of pathological α-syn, tau and Aβ aggregates in tissue sections from α-synucleinopathy, tauopathies and control donors was confirmed by immunostaining.

In Vitro Competition (K_i) Assays

The equilibrium inhibition constant (K_i) values of the unlabelled compounds (asyn-44 derivatives as well as tau ligands) were determined versus tritium-labelled asyn-44 according to our published methods.[21] Frozen aliquots (−80 °C) of homogenized human PD (asyn-44 derivatives) or AD (tau ligands) tissue (10 mg/mL in phosphate buffered saline) were thawed and diluted in 50 mM tris buffer (pH = 7.0) to 1 mg/mL. The unlabelled competitors were dissolved in DMSO at a concentration of 400 µM and diluted to 20 µM with tris buffer, resulting in a 5% DMSO solution in tris buffer. The subsequent serial dilution (6 µM to 4 nM) was made with 5% DMSO in tris buffer to maintain a constant DMSO concentration. 50 µL of the respectively diluted solution was added to 50 µL of [^{3}H]asyn-44 and 800 µL of tris buffer/20% ethanol/0.1% bovine serum albumin (BSA), resulting in concentrations of 1 nM [^{3}H]asyn-44 and 0.2-1000 nM unlabelled

10.1002/chem.202303921

competitor. To this, 100 µL of the 1 mg/mL brain homogenate was added (100 µg/mL final tissue concentration) and the mixture was incubated for 60 min at room temperature, filtered through a Whatman GF/B glass filter via a Brandel M-24R cell harvester (Gaithersburg, MD, USA) and rapidly washed three times with 3 mL of tris buffer/20% ethanol/0.1% BSA. The filters were counted in CytoScint-ES after thorough vortexing. The concentration of bound compound was determined from the radioactivity retained on the filter (corrected for nonspecific binding (*vide infra*)) and the molar activity of the tritiated compound.

The equilibrium inhibition constant (K_i) values of the unlabelled asyn-44 was determined in AD brain homogenates versus tritium-labelled Pittsburgh compound B according to our published methods.[28] Essentially, a similar procedure was carried out as outlined for [^{3}H]asyn-44 using PBS instead of tris buffer.

Two Point Screening Assays

Screening assays of test compounds were conducted at concentrations of 30 and 300 nM unlabelled competitor in PD brain homogenate versus tritium-labelled asyn-44. The assay was carried out similarly as described for the K_i assay (*vide supra*). No (0%) inhibition was defined by the number of counts without the addition of any unlabelled competitor and complete (100%) inhibition was defined as the number of counts at 1 µM of the unlabelled radioligand (nonspecific binding). The % inhibition of the radioligand by the test compound at 30 or 300 nM was defined by the number of counts specifically bound at 30 or 300 nM divided by the difference of counts at 0% inhibition minus the counts at 100% inhibition multiplied by 100. All assays were performed in triplicate at each concentration.

Equilibrium dissociation constant (K_d) and B_{max} assays

Tritium-labelled asyn-44 homologous binding assays utilized PD, AD, or control brain homogenates to determine equilibrium dissociation constant (K_d) and B_{max} values and were performed as previously described with minor modification, which included the use of a binding assay and filter wash solutions of tris buffer (50 mM, pH 7.0)/20% ethanol/0.1% BSA.[21]

Autoradiography

In vitro autoradiography was performed using 6-µm-thick deparaffinized sections derived from MSA, PD, AD, CBD, PSP and CT brains. Brain sections were first equilibrated for 20 min in PBS (Dulbecco's phosphate buffered saline) and then incubated with 4 nM [^{3}H]asyn-44 (specific activity 34 Ci/mmol) in assay binding buffer (PBS + 20% EtOH) for 90 min at RT. To determine the non-specific binding (NSB), adjacent brain sections were incubated with [^{3}H]asyn-44 mixed with 10 µM of unlabelled asyn-44. After incubation, slides were washed 3 x 5 min in cold washing buffer (PBS + 20% EtOH) to remove unbound tracer and then dipped briefly in distilled water. Slides were then allowed to air-dry before being exposed and scanned in a real-time autoradiography system (BeaQuant instrument, ai4R) for 5 h. ROI delimitation and quantification of signal was performed by using the image analysis software Beamage (ai4R). Specific binding was determined by subtracting the non-specific signal from the total signal and expressed as counts/min/mm^2. Immunohistochemistry was performed on deparaffinized sections adjacent to those used for autoradiography. Sections were permeabilized with 0.1% Triton™ X-100 for 10 min followed by 3 x 5 min washes in PBS Tween20 buffer. Sections underwent hydrogen peroxide blocking for 15 min and PBS + 10% goat serum + 1% BSA + 0.1% Tween 20 blocking for 1 h at room temperature. Sections were immunostained using α-syn (phosphor S129) antibody (P-syn/81A) (Abcam), anti-phospho-tau (Ser202, Thr205) antibody (ThermoFisher), used at 1:500 dilution overnight at 4 ºC. After a series of thorough washes with PBST buffer, the slides were incubated with the secondary antibodies Goat Anti-Mouse IgG H&L (HRP) (Abcam) at 1:10000 for 1 h at room temperature. The sections were washed again with PBST buffer for 3 x 5 min, treated with DAB substrate for 10 min and counterstained by Meyer's hematoxylin dye. Subsequently, the sections were mounted with Limonene mounting media and coverslips for microscopy. Images were captured with a Zeiss microscope at 10X magnification.

PET imaging

A total of 6 healthy adult rats (Sprague Dawley, 4-month old, 364±88 g; 3/3 M/F) underwent PET imaging following bolus injection of [^{18}F]asyn44. Rats were catheterized in the tail vein and positioned in a dedicated small animal PET/CT scanner (nanoScan™, Mediso Ltd., Budapest, Hungary). Anaesthesia was maintained throughout the scanning period while monitoring body temperature and respiration. A computed tomography (CT) was acquired before each PET scan and used for attenuation and scatter correction purposes as well as PET/CT co-registration and co-registration with a stereotactic MR atlas of rat brain[29] to define anatomical regions of interest (ROI). Dynamic PET scans were acquired for 120 minutes immediately after i.v. administration of [^{18}F]asyn-44 (18.3±1.8 (16.5-21.1) MBq, 0.19-1.05 nmol/kg, 54-268 GBq/µmol).

The acquired list mode data were sorted into 39 frames (3 × 5, 3 × 15, 3 × 20, 7 × 60, 17 × 180, and 6 × 600 s) 3D true sinograms (ring difference 84). The 3D sinograms were converted into 2D sinograms using Fourier-rebinning and reconstructed using a 2D-filtered back projection (FBP) with a Hann filter at a cut-off of 0.50 cm^{-1}. Static images of the complete emission acquisition and different time frames of 0-5, 5-60 and 60-120 min were reconstructed with the manufacturer's proprietary iterative 3D algorithm (six subsets and four iterations). All image data were corrected for detector geometry and efficiencies, dead-time and decay-corrected to the start of acquisition, with corrections for attenuation and scatter using a CT-based material map. Image analyses and extraction of brain TACs from the dynamic FBP images were performed using VivoQuant® 2020 (2020patch1, Invicro, Needham, MA, USA). Standardized uptake values (SUV) were calculated by normalizing the regional radioactivity for injected radioactivity and body weight of the animal.

Metabolites

[^{18}F]Asyn-44 (19-48 MBq) was injected into the tail vein of healthy Sprague Dawley rats (5-8-month old, 409±96 g; 6/5 M/F) under isoflurane anaesthesia. The animals were recovered from anaesthesia after tracer injection and at 30 and 60 minutes post injection, they were sacrificed by decapitation and trunk blood samples were collected in heparinised tube (n=2-3 for each time point) and centrifuged at 2,500 RCF (Relative centrifugal force) for 5 min to collect plasma. Brains were excised quickly and homogenized with a BeadBug™ (Benchmark Scientific; Sayreville, NJ, USA) in 3.2 mL ice-cold acetonitrile together with 1 µg of unlabelled parent compound to facilitate tracer extraction, then 1.6 mL deionized water was added and mixed. The homogenate was centrifuged at 12,000 g for 5 min and the supernatant was collected. Plasma and brain extract were analysed by column-switching HPLC on a Luna C18(2) column (10 µm, 4.6 × 250 mm, Phenomenex) with mobile phase of 40:60 CH_3CN/ 0.1 M ammonium formate in water at 2 mL/min. The HPLC data was analyzed with PowerChrom chromatography software (eDAQ Pty Ltd.; Colorado Springs, Colorado, US).

Acknowledgements

We thank Dr. Jamie Eberling and Dr. Glenn Harris for helpful discussions, and Manik Debnath for technical support with the binding assays. We also thank the members of Novandi Chemistry AB, the CAMH Brain Health Imaging Centre, and the University of Pittsburgh PET Facility for their support.

A.P. thanks CAMH for postdoctoral fellowships from the Discovery Fund and *womenmind*™. C.A.M. and N.V. thank the Michael J. Fox Foundation and the Rainwater Charitable Foundation (Tau Consortium) for supporting this research collaboration. R.H.M., C.A.M., and N.V. thank the National Institute on Neurological Disorders and Stroke (NINDS) for supporting this research collaboration (U19 NS110456). N.V. also thanks the Azrieli Foundation, the Canada Research Chairs Program, Canada Foundation for Innovation and the Ontario Research Fund for financial support.

Human brain tissue samples were provided by the Neurodegenerative Disease Brain Bank at the University of California, San Francisco (which receives funding support from NIH grants P30AG062422, P01AG019724, U01AG057195, and U19AG063911, the Rainwater Charitable Foundation, and the Bluefield Project to Cure FTD) and by the Banner/Sun Health Brain Bank funded by the Michael J. Fox Foundation.

Keywords: α-synuclein• positron emission tomography • Parkinson's disease • fluorine-18

[1] A. Maurer, A. Leonov, S. Ryazanov, K. Herfert, L. Kuebler, S. Buss, F. Schmidt, D. Weckbecker, R. Linder, D. Bender, A. Giese, B. J. Pichler, C. Griesinger, *ChemMedChem* **2020**, *15*, 411–415.
[2] M. X. Henderson, J. Q. Trojanowski, V. M.-Y. Lee, *Neuroscience Letters* **2019**, *709*, 134316.
[3] C. A. Mathis, B. J. Lopresti, M. D. Ikonomovic, W. E. Klunk, *Seminars in Nuclear Medicine* **2017**, *47*, 553–575.
[4] Š. Korat, N. S. R. Bidesi, F. Bonanno, A. Di Nanni, A. N. N. Hoàng, K. Herfert, A. Maurer, U. M. Battisti, G. D. Bowden, D. Thonon, D. Vugts, A. D. Windhorst, M. M. Herth, *Pharmaceuticals* **2021**, *14*, 847.
[5] P. T. Kotzbauer, Z. Tu, R. H. Mach, *Clin Transl Imaging* **2017**, *5*, 3–14.
[6] C. K. Nwabufo, O. P. Aigbogun, *J Neurol* **2022**, *269*, 5762–5786.
[7] M. Sevenich, D. Honold, A. Willuweit, J. Kutzsche, J. Mohrlüder, D. Willbold, *Neurochemistry International* **2022**, *161*, 105422.
[8] A. Kallinen, M. Kassiou, *Nuclear Medicine and Biology* **2022**, *114–115*, 115–127.
[9] D. J. Irwin, H. I. Hurtig, *J Alzheimers Dis Parkinsonism* **2018**, *08*, DOI 10.4172/2161-0460.1000444.
[10] J. Xiang, Y. Tao, Y. Xia, S. Luo, Q. Zhao, B. Li, X. Zhang, Y. Sun, W. Xia, M. Zhang, S. S. Kang, E.-H. Ahn, X. Liu, F. Xie, Y. Guan, J. J. Yang, L. Bu, S. Wu, X. Wang, X. Cao, C. Liu, Z. Zhang, D. Li, K. Ye, *Cell* **2023**, *186*, 3350-3367.e19.
[11] J. P. Seibyl, *J Nucl Med* **2022**, *63*, 1463–1466.
[12] O. M. Alzghool, G. Van Dongen, E. Van De Giessen, L. Schoonmade, W. Beaino, *Movement Disorders* **2022**, *37*, 936–948.
[13] H. Y. Kim, W. K. Chia, C.-J. Hsieh, D. Saturnino Guarino, T. J. A. Graham, Z. Lengyel-Zhand, M. Schneider, C. Tomita, M. G. Lougee, H. J. Kim, V. V. Pagar, H. Lee, C. Hou, B. A. Garcia, E. J. Petersson, J. O'Shea, P. T. Kotzbauer, C. A. Mathis, V. M.-Y. Lee, K. C. Luk, R. H. Mach, *J. Med. Chem.* **2023**, *66*, 12185–12202.
[14] A. Di Nanni, R. S. Saw, U. M. Battisti, G. D. Bowden, A. Boeckermann, K. Bjerregaard-Andersen, B. J. Pichler, K. Herfert, M. M. Herth, A. Maurer, *ACS Omega* **2023**, *8*, 31450–31467.
[15] R. Smith, F. Capotosti, M. Schain, T. Ohlsson, E. Vokali, J. Molette, T. Touilloux, V. Hliva, I. K. Dimitrakopoulos, A. Puschmann, J. Jögi, P. Svenningsson, M. Andréasson, C. Sandiego, D. S. Russell, P. Miranda-Azpiazu, C. Halldin, E. Stomrud, S. Hall, K. Bratteby, E. Tampio L'Estrade, R. Luthi-Carter, A. Pfeifer, M. Kosco-Vilbois, J. Streffer, O. Hansson, *Nat Commun* **2023**, *14*, 6750.
[16] L. Kuebler, S. Buss, A. Leonov, S. Ryazanov, F. Schmidt, A. Maurer, D. Weckbecker, A. M. Landau, T. P. Lillethorup, D. Bleher, R. S. Saw, B. J. Pichler, C. Griesinger, A. Giese, K. Herfert, *Eur J Nucl Med Mol Imaging* **2021**, *48*, 1759–1772.
[17] J. Molette, E. Gabellieri, V. Darmency, *Bicyclic Compounds for Diagnosis and Therapy*, **n.d.**, WO 2017/153601 A1.
[18] J. Molette, *Novel Compounds for Diagnosis*, **n.d.**, WO 2021/224489 A1.
[19] A. A. Wilson, L. Jin, A. Garcia, J. N. DaSilva, S. Houle, *Applied Radiation and Isotopes* **2001**, *54*, 203–208.
[20] A. Lindberg, M. Chassé, C. Varlow, A. Pees, N. Vasdev, *Labelled Comp Radiopharmac* **2023**, *66*, 205–221.
[21] T. J. A. Graham, A. Lindberg, J. Tong, J. S. Stehouwer, N. Vasdev, R. H. Mach, C. A. Mathis, *J. Med. Chem.* **2023**, *66*, 10628–10638.
[22] K. L. Kirk, C. R. Creveling, *Medicinal Research Reviews* **1984**, *4*, 189–220.
[23] C. Ni, J. Hu, *Chem. Soc. Rev.* **2016**, *45*, 5441–5454.
[24] V. W. Pike, *Trends in Pharmacological Sciences* **2009**, *30*, 431–440.
[25] K. K. Ghosh, P. Padmanabhan, C.-T. Yang, S. Mishra, C. Halldin, B. Gulyás, *EJNMMI Res* **2020**, *10*, 109.
[26] P. R. Lazzara, T. W. Moore, *RSC Med. Chem.* **2020**, *11*, 18–29.
[27] D. J. St. Jean, C. Fotsch, *J. Med. Chem.* **2012**, *55*, 6002–6020.
[28] W. E. Klunk, Y. Wang, G. Huang, M. L. Debnath, D. P. Holt, L. Shao, R. L. Hamilton, M. D. Ikonomovic, S. T. DeKosky, C. A. Mathis, **n.d.**
[29] A. J. Schwarz, A. Danckaert, T. Reese, A. Gozzi, G. Paxinos, C. Watson, E. V. Merlo-Pich, A. Bifone, *NeuroImage* **2006**, *32*, 538–550.

10.1002/chem.202303921

WILEY VCH

RESEARCH ARTICLE

Entry for the Table of Contents

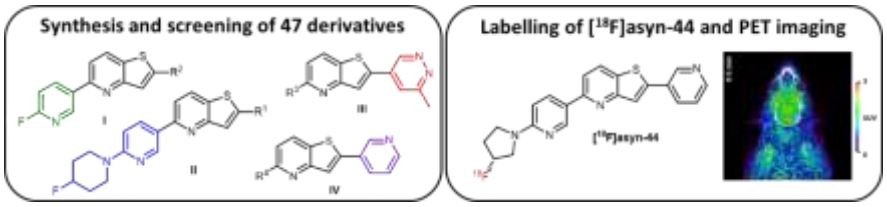

47 derivatives of a potent α-synuclein aggregate binding pyridothiophene (asyn-44) were synthesized and screened against [^{3}H]asyn-44 in competitive binding assays using post-mortem Parkinsons disease brain homogenates and K_i values of the most potent compounds were determined. Asyn-44 was labelled with fluorine-18 for preliminary PET imaging in rats, which showed high initial brain uptake, moderate washout, and low variability.